Study Book
EMSCULPT neo®

EMSCULPTNEO.COM
SALES@BTLNET.COM

Please be aware that some of the information / intended uses / configurations / accessories mentioned here are not available in your country. For more information contact your local distributor. **Results and patient experience may vary.** As with any medical procedure, ask your doctor if the EMSCULPT NEO® procedure is right for you. In the EU EMSCULPT NEO® is intended for treatment of obesity by fat reduction through neuromuscular stimulation, radiofrequency induced lipolysis and increase of the blood flow. *Data on file.

04/2021


EMSCULPT neo
EMSCULPT


EMSCULPT neo


EMSCULPT neo


EMSCULPT
neo


EMSCULPT
neo

American Journal of
Biomedical Science & Research

www.biomedgrid.com
ISSN: 2642-1747

Mini review

A Novel Technology Combining RF and Magnetic Fields: Technical Elaboration on Novel RF Electrode Design

Diane Duncan*, M.D., FACS

Plastic Surgical Associates, Fort Collins CO, USA

***Corresponding author:** Diane Duncan, M.D., FACS, Plastic Surgical Associates, Fort Collins CO, 1701 East Prospect Road, USA.

To Cite This Article: *Diane Duncan, A Novel Technology Combining RF and Magnetic Fields: Technical Elaboration on Novel RF Electrode Design. 2020 - 11(1). AJBSR.MS.ID.001608.* DOI: 10.34297/AJBSR.2020.11.001608.

Received: November 28, 2020; **Published:** December 08, 2020

Abstract

The article provides an insight into the technological aspects of a novel technology in body shaping allowing simultaneous delivery of HIFEM magnetic fields and radiofrequency energy. The device utilizes circular coil for magnetic field induction and radiofrequency electrodes in a single applicator which poses a technological challenge to the construction. To overcome the challenges a novel electrode design has been introduced for avoiding interferences between the two types of energy. As such the device presents a shift in the body contouring segment of aesthetic medicine, because it allows a simultaneous treatment of muscle laxity through supramaximal muscle stimulation and reduction of excessive adipose tissue through radiofrequency heating.

Keywords: HIFEM, Radiofrequency, Synchrode RF Electrode, Body Contouring

Abbreviations: HIFEM: High Intensity Focused Electromagnetic Field; RF: Radio Frequency

Introduction

In aesthetic medicine, various technologies are used for non-invasive body shaping. Two of the most widely used modalities are radiofrequency heating of tissues and high-intensity electromagnetic muscle activation. These two principles represent energy application arising from two different frequency bands of the electromagnetic spectrum within humans. Radio frequency (RF) are waves in the frequency range of roughly 20 kHz to 300 GHz. These are the frequencies with the ability to create heat through the oscillation of molecules while propagating within the tissue. In the aesthetic medicine, the RF energy is usually emitted by a solid metal electrode, which is normally in direct contact with the patient. The heating effects of the RF technology can be used for wide range of applications such as fat cell disruption, skin tightening or cellulite reduction [1-3]. For muscle activation, a high-intensity electromagnetic field (HIFEM) is used. The HIFEM field represents a very-low frequency range (<10kHz).

During the application, rapid alternations in the magnetic field induce a secondary electric current in the tissue. These currents do not create any heat but are able to both polarize and depolarize the motor neurons that innervate the muscle, thus eliciting muscle contractions of supramaximal nature that cannot be achieved voluntarily. Such stimulation was found to result in muscle hypertrophy [4-6]. To emit HIFEM energy for muscle activation, an applicator with an embedded round metal coil is used without direct contact with the patient. Until recently, these two energies have been used solely as standalone modalities, and their combination in close-space engineering would be restricted by physical laws, due to frequency incompatibility and technical interference. However, the latest breakthrough in the field presented a technological solution overcoming these issues. The main goal of this article is thus to describe and explain the technical aspects of this innovation. Technical issues associated with simultaneous HIFEM and RF application In order to apply both RF and HIFEM at the same time within the same location, the metal RF electrode and the magnetic coil generating HIFEM field would need to be incorporated in a single applicator that is in contact with the patient.

However, while the magnetic fields easily pass through most common materials such as wood, plastic or even human tissue,

they cannot pass through metal without mutual interactions. Any metals, when exposed to rapidly changing HIFEM fields quickly heat up (see Picture 1) and also tend to be physically repulsed. For this same reason, HIFEM is strictly contraindicated in patients with metal and electronic implants. With this known contraindication, HIFEM and ordinary RF can't be emitted simultaneously within the same field without overheating the metal electrode generating RF as the electrodes are made of a solid metal. Although the RF electrodes are used to generate heat, their overheating could result in malfunctions in the RF delivery but most importantly would expose the patient to risk of burns. An evidence of the heating effect can be seen in the Figure 1 where metal plates are placed over the magnetic coil applicator (Figure 1).

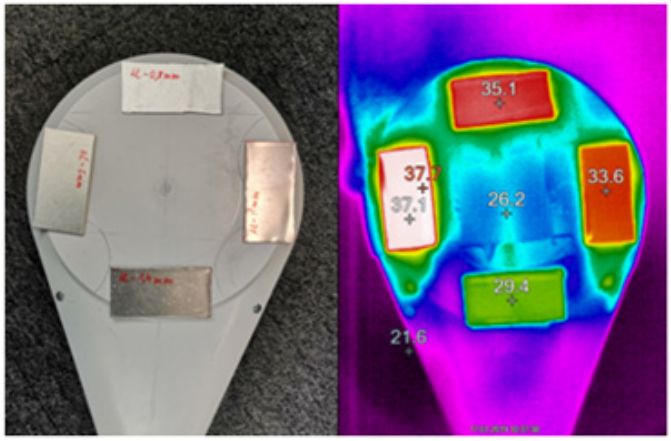

Figure 1: Digital photographs of running applicator containing the circular coil and metal plates placed over. The right image shows the metal plates' temperature elevation as captured by the thermal camera.

Technical solution allowing simultaneous application

To enable HIFEM to pass through the electrode without this heating phenomenon an entirely new electrode technology has been developed and patented by a leading company in the aesthetic market (BTL Industries Inc., Boston MA). While solid electrodes represent an issue for the magnetic field, the patented Synchrode RF electrode uses a special design concept which makes it transparent to the HIFEM energy. Instead of using a single coherent metal structure, the Synchrode RF electrode is comprised of 56 smaller segment pairs, with each segment pair laid out close to each other, creating individual positive and negative (+/-) RF poles (112 segments per applicator). The main purpose for using this segmented design and for having multiple interspacings is to achieve selective tissue heating effects as with large-sized solid electrode but without the technical limitations associated with a solid electrode (see Figure 2). The device utilizing this technology offers two treatment applicators, allowing a total of 224 interspaced electrode segments to work in synchrony during the treatment (Figure 2).

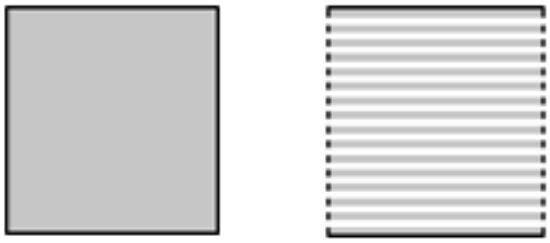

Figure 2: Illustration of the difference between standard and segmented electrode. Standard electrodes are made of compact material as a single piece (left), while the segmented electrode is composed of multiple interspaced segments (right).

The key to this breakthrough technology is the interspacing. This interspaced design allows the HIFEM to pass through the electrode easily without any unfavorable interaction with its metal parts. Instead, the electrode is transparent to the magnetic fields, allowing them to continue in their intended direction (See Figure 3). Through years of development and testing, the Synchrode RF electrode's overall size and shape is specifically tailored to work in synchrony with the HIFEM magnetic fields. The electrode design takes into consideration the exact shape, the depth of penetration, as well as the intensity of HIFEM fields. The magnetic coil and the Sychrode RF electrode are thus truly synchronized with each other from an engineering standpoint (Figure 3).

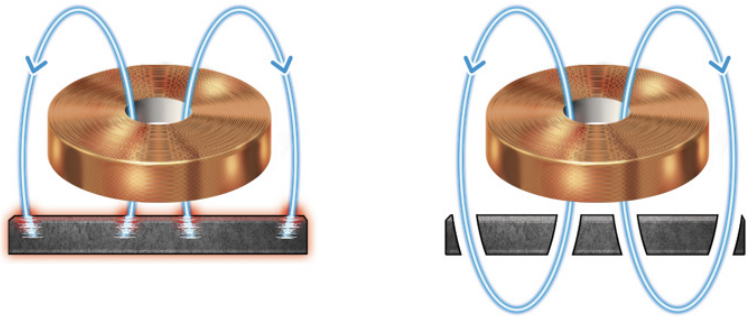

Figure 3: Illustration of the mutual interaction between magnetic coil and underlying electrode. The interspaced electrode is transparent to the HIFEM's magnetic field and the magnetic waves can pass without interaction, while standard electrode absorbs the HIFEM energy, resulting in heat.

Conclusion

For the very first time in the aesthetic field, this patented concept allows practitioners to simultaneously apply RF heating and high-intensity electromagnetic muscle (HIFEM) activation in the same treatment area, at the same time. This represents an engineering breakthrough that now allows leveraging both the clinical, as well as commercial synergies of combining two gold standard technologies from a single device applicator. The company holding the patent rights (BTL Industries Inc., Boston MA) has already implemented this solution in a novel body shaping device introduced in October 2020 (EMSCULPT NEO) and presented the results of several clinical studies showing synergistic effects on muscle and fat tissues [7-10]. Although this electrode design solution has been first used for body shaping where it shows superior results, its' use may not be limited only to aesthetic medicine but could found a variety of other applications in another medical areas such as physiotherapy or rehabilitation.

Conflict of Interest

Dr. Diane Duncan is medical advisor for BTL, no funding was received for this article.

References

1. Angélica Rodrigues de Araújo, Viviane Pinheiro Campos Soares, Fernanda Souza da Silva, Tatiane da Silva Moreira (2015) Radiofrequency for the treatment of skin laxity: mith or truth. Anais Brasileiros de Dermatologia 90(5): 707-721.
2. Alizadeh Z, Halabchi F, Mazaheri R, Abolhasani M, Tabesh M, et al. (2016) Review of the Mechanisms and Effects of Noninvasive Body Contouring Devices on Cellulite and Subcutaneous Fat. Int J Endocrinol Metab 14(4): e36727.
3. Emilia del Pino M, Rosado RH, Azuela A, Ma Graciela Guzmán, Dinorah Argüelles, et al. (2006) Effect of controlled volumetric tissue heating with radiofrequency on cellulite and the subcutaneous tissue of the buttocks and thighs. J Drugs Dermatol JDD 5(8): 714-722.
4. Duncan D, Dinev I (2019) Noninvasive Induction of Muscle Fiber Hypertrophy and Hyperplasia: Effects of High-Intensity Focused Electromagnetic Field Evaluated in an In-Vivo Porcine Model: A Pilot Study. Aesthet Surg J 40(5): 568-574.
5. Kinney BM, Lozanova P (2019) High intensity focused electromagnetic therapy evaluated by magnetic resonance imaging: Safety and efficacy study of a dual tissue effect based non-invasive abdominal body shaping. Lasers Surg Med 51(1): 40-46.
6. Kent DE, Jacob CI (2019) Simultaneous Changes in Abdominal Adipose and Muscle Tissues Following Treatments by High-Intensity Focused Electromagnetic (HIFEM) Technology-Based Device: Computed Tomography Evaluation. J Drugs Dermatol JDD 18(11): 1098-1102.
7. Weiss RA, Bernardy J, Tichy F (2020) Radiofrequency treatment used in combination with HIFEM therapy: Histological analysis includin scanning electron microscopy of adipocytes. Lasers Surg Med 52(S32): S5-S82.
8. Halaas Y, Bernardy J, Ondrackova P, Dinev I (2020) The skeletal muscle satellite cell activation by a combination of HIFEM procedure and radiofrequency treatment for body contouring: A first look at the NCAM/CD56 facilitated detection by fluorescent microscopy. In: ASDS 2020.
9. Katz BE, Samuels JB, Weiss RA (2020) Novel Radiofrequency Device Used in Combination with HIFEM Procedure for Abdominal Body Shaping: Sham-Controlled Randomized Trial. In: ASDS 2020.
10. Jacob C, Kent DE (2020) Abdominal Toning and Reduction of Subcutaneous Fat with Combination of HIFEM Procedure and Radiofrequency Treatment. In: ASDS 2020.

Simultaneous Application of High-Intensity Focused Electromagnetic and Synchronized Radiofrequency for Fat Disruption: Histological and Electron Microscopy Porcine Model Study

Robert A. Weiss, MD, FAAD,* Jan Bernardy, PhD,† and Frantisek Tichy, CSc‡

BACKGROUND Radiofrequency (RF) and high-intensity focused electromagnetic (HIFEM) technologies are used for noninvasive body shaping as standalone modalities.

OBJECTIVE To examine the effects of novel synchronized RF and HIFEM on subcutaneous adipose tissue in a porcine animal model.

MATERIALS AND METHODS Seven large white pigs aged 6 months received 3 abdominal treatments of simultaneous application of synchronized RF and HIFEM (30 minutes, once per week). Punch biopsies of treated and control subcutaneous tissue were collected at the baseline, 4 days, 2 weeks, 1 month, and 2 months. Specimens were examined by light and scanning electron microscopy. Adipocyte volume was analyzed. Fat tissue temperature was measured in situ (fiber optic probes) and superficially (thermal imager).

RESULTS Fat layer was heated to temperatures of 42 to 45°C. Signs of fat apoptosis (shape alternations and pyknotic nuclei) appeared at day 4 and peaked between 2 weeks and 1 month. Adipocyte volume decreased significantly ($p < .001$) by 31.1% at 2 weeks, 1 month (−23.6%), and 2 months (−22.0%). Control samples showed healthy adipocytes. Scanning electron microscopy micrographs corroborated histology findings, showing flattened, volume-depleted and disrupted adipocytes.

CONCLUSION Synchronized RF with HIFEM procedure resulted in a significant and sustained fat reduction with no adverse events.

Noninvasive techniques for body shaping as an alternative to the invasive methods are generally sought and well accepted by the public because they pose less risk with minimum side effects and no downtime.[1] Novel synchronized radiofrequency (RF) and high-intensity focused electromagnetic (HIFEM) technologies were recently developed to provide noninvasive body shaping using heat and intensive muscle contractions, respectively.

The effect of RF technology is based on generating heat in different tissues through the transformation of RF energy into heat.[2] Certain frequencies of the RF spectrum allow for selective heating of skin or subcutaneous adipose tissue because of the different dielectric properties of biological tissues. Hence, RF is often used for fat removal, skin tightening, or cellulite reduction.[3–8]

From the *Maryland Laser Skin, & Vein Institute, Hunt Valley, Maryland; †Veterinary Research Institute, Brno, CZ; ‡Department of Anatomy and Histology, Faculty of Veterinary Medicine, University of Veterinary and Pharmaceutical Sciences Brno, CZ

R.A. Weiss receives research grants from BTL. The other authors have indicated no significant interest with commercial supporters.

Address correspondence and reprint requests to: Robert Weiss, MD, Maryland Laser Skin & Vein Institute, 54 Scott Adam Rd Ste 301, Aspen Mill Professional Building, Hunt Valley, MD 21030 CA 90212, or e-mail: rweiss@mdlsv.com

http://dx.doi.org/10.1097/DSS.0000000000003091

High-intensity focused electromagnetic technology induces muscle contractions through stimulation of the nerve pathways. The magnetic field induces electric currents, depolarizing the cell membranes of nerve cells to propagate an action potential and contract muscle fibers.[9] Intense muscle contractions (referred to as supramaximal) result in an increase in the muscle mass through hypertrophy/hyperplasia.[10]

Noninvasive fat reduction requires lipolysis, which is the breakdown of triglycerides stored in the fat cells into glycerol and free fatty acids (FFAs). Radiofrequency-targeted heating of subcutaneous tissue results in increased fat cell metabolism, which facilitates this breakdown.[11,12] In addition, a simultaneous intensive muscle workload, such as during HIFEM treatment, is accompanied by an elevated level of lipolysis due to the increased local energy consumption.[13]

For long-term reduction of subcutaneous fat tissue, necrosis or apoptosis must be achieved and seen on histological studies.[11] Necrosis is immediate cell death that can follow various external factors, such as excessive heat, cold, and toxins, and can lead to untoward side effects.[14,15] It is usually linked with intensive inflammation and possible panniculitis (e.g., significant lymphohistiocytic infiltrate).[16,17] By contrast, apoptosis, a process by which the body replaces old/damaged cells, manifests itself with very mild immune response[18,19] and is therefore known as the

"silent cell death." Importantly, it has been shown that apoptosis is usually a temperature-dependent event. With a minimal 15-minute exposure time, apoptosis can be initiated with temperatures of 42°, and exposure time to trigger apoptosis decreases as the temperature rises. Apoptosis is achieved with temperatures of up to 45°C, whereas higher temperatures may result in immediate cell death or necrosis.[11,20–22] Regarding necrosis versus apoptosis, necrosis is immediate death of tissue that can cause a whole host of problems including panniculitis and should be avoided. Apoptosis is a slow programmed death that is associated with less side effects and is preferable.

When applying RF and HIFEM simultaneously, a primary effect on fat tissue is attributed to the RF-heating–induced apoptosis. Hypothetically, the use of a dual-modality approach might boost the metabolic activity for more effective fat reduction. High-intensity focused electromagnetic contractions might also aid with heat distribution and reduce risk of hot spots.[23,24]

Technical limitations have previously prevented the concurrent use of HIFEM and RF technology because of the interference between 2 competing electromagnetic fields. This study describes a novel synchronized RF that allows simultaneous combination of both technologies. In this porcine study, the use of HIFEM and synchronized RF determines effects on adipose tissue using both H&E histology and scanning electron microscopy (SEM).

Materials and Methods

An institutional review board approved this prospective animal study of 7 large white pigs (females) aged approximately 6 months. The number of animals was chosen to respect the 3Rs principle for animal experimentation as much as possible, and the study was performed in accordance with the EU Directive for animal experiments. A certified veterinarian supervised all the procedures.

All animals received active treatment 1 week after the acclimatization period. Three 30-minute abdominal therapies once a week for 3 weeks per pig were performed using Emsculpt Neo device (BLT Industries Inc., Boston, MA), which simultaneously combines novel synchronized RF and HIFEM technologies in a single applicator. The applicator was placed on the abdominal area, affixed by a fixation belt, and therapy power was set to maximum allowed intensity for both modalities. Animals were under general anesthesia. Before each therapy, anesthetic premedication was performed by the mixture of tiletamine 2 mg/kg, zolazepam 2 mg/kg, ketamine 2 mg/kg, and xylazine 2 mg/kg. During the therapy, anesthesia was maintained because of the continual influx of 2% propofol solution (1–2 mg/kg) by a cannula inserted into the auricular vein. The vital functions of animals were monitored during the therapy.

Using ultrasound guidance (Mindray M5Vet, probe 10L4s), a flexible fiber optic temperature probe (LumaSense Technologies Inc., Raunheim, Hessen, Germany) was inserted into the subcutaneous fat tissue just below the applicator (the middepth of the fat layer) to monitor in situ the temperatures of the adipose tissue during the therapy (Figure 1). The superficial skin temperature was monitored immediately after removing the applicator at the end of the procedure by a thermal imaging camera (Fluke Ti300, Fluke Corporation).

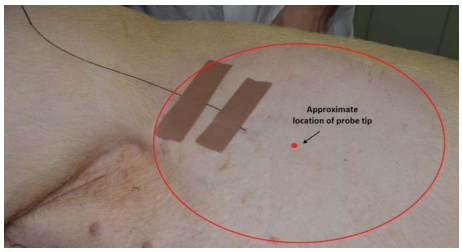

Figure 1. Fiber optic temperature probe inserted into the mid-depth of subcutaneous tissue. The probe tip (red dot) was located in the center of the shaved treated area (circled). The fiber was fixed by an adhesive tape to prevent its displacement during the therapy.

Biopsy specimens of the fat tissue for histological and SEM examination were collected at baseline, 4 days (D4), 2 weeks (W2), 1 month (M1), and 2 months (M2) posttreatment for each animal by biopsy punch (6 mm in diameter). Two specimens per time point (one for histology and one for SEM) were collected from the treatment site. Control specimens of abdominal fat tissue were collected from the opposite side of each subject animal.

For histological examination, hematoxylin and eosin (H&E) staining was used. In total, 252 tissue slices were analyzed. The samples for SEM were fixed with 3% paraformaldehyde and 2% glutaraldehyde and then gold stained. Micrographs were taken using a JSM-6380LV microscope (Jeol Ltd, Akishima, Japan). Expert evaluation of all slices and micrographs in a random order was performed by an experienced histopathologist.

Adipocyte cross-sectional area measurements were made using ImageJ v1.52p software. The area of fat cells was calculated for each analyzed image. Descriptive statistics (mean and SD) were used to identify the change in adipocyte size. Significance of this change was analyzed by one-way analysis of variance, followed by the Tukey–Kramer post hoc test. A p value less than 0.05 was accepted as the level of statistical significance.

Results

Clinical examination during all phases showed normal health of all animals, and no complications regarding animal care occurred. Animals always recovered well from the anesthesia procedure without any treatment-related complications or side effects.

Temperature Measurements

Subcutaneous fat temperature measured in situ reached 42°C in the first 4 minutes (Figure 2). Then 44°C was reached soon after, and for the rest of the procedure (23 minutes), temperature was maintained in a 44 to 45°C range. The skin temperature measured immediately after the treatment showed safe values between 42°C and 43°C in all animals.

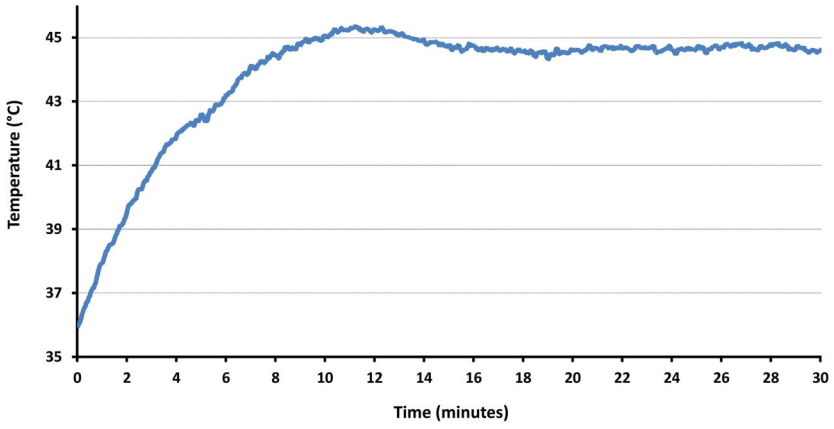

Figure 2. Continuous temperature measurement by the fiber optic probe located in the middle of fat tissue layer depth (Pig No. 3; first therapy, RF, and HIFEM set to maximum allowed intensity). The therapeutic temperature was achieved in the first 4 minutes, and it was maintained at a stable level of 44 to 45°C, during most of the procedure. HIFEM, high-intensity focused electromagnetic; RF, radiofrequency.

Histology Evaluation

Baseline and control samples showed predominantly normal round/polygonal-shaped healthy adipocytes without any damage to fat tissue (Figure 3). Four days after the last treatment, alternations of the cell shape were present. Adipocytes were noticeably flattened and of a smaller size ($p < .001$; Figure 3) with multiple adipose cells showing membrane rupture. Connective tissue (collagen fibers) shows conformational changes. Initiation of a mild inflammatory response was also observed with some neutrophils, lymphocytes, and macrophages seen perivascularly and surrounding adipocytes. The presence of subtle infiltration by these cells indicated that the elimination of damaged fat cells had already been initiated.

Two weeks after the final treatment, adipocytes were flattened and of significantly ($p < .001$) smaller size because of the release of their lipid content caused by the lipolytic effect of the simultaneous application of RF and HIFEM therapy (Figures 3 and 5). Multiple adipocyte nuclei demonstrated pyknotic appearance (a sign of apoptotic changes), as evidenced by their small and shrunk nuclei with dark, highly condensed nuclear chromatin. Furthermore, some membranes manifested rupture with unusual shape alternations, whereas immune cells were observed perivascularly. Macrophages (foamy histiocytes) and lipophages could be seen in areas where the damaged fat cells were being cleared.

One month after the last treatment, unstructured spaces of various sizes were present, caused by the elimination of fat cells (Figure 4). Ruptures in some adipocyte membranes were still visible. The inflammatory infiltrate receded, indicating that the removal of damaged tissue peaked in between 14 and 30 days. The diameter of the intact adipocytes was below the baseline values because they seemed to contain less lipids than pretreatment ($p < .001$; Figure 5).

At 2 months, the inflammatory infiltrate was occasionally present as a part of late tissue healing response along with a few ruptured membranes of adipocytes (Figure 4). Adipocytes showed no major alterations in shape but still remained smaller compared with the baseline ($p < .001$). In addition, as a result of the collagen remodeling induced by the RF,[25] the interlobular septa seemed well-developed. Notably, no damage to the blood vessels or necrosis of the fat tissue was observed.

Area of Adipocytes

Treated adipocytes showed a smaller diameter than at baseline (Figure 5). Overall, the fat tissue showed a

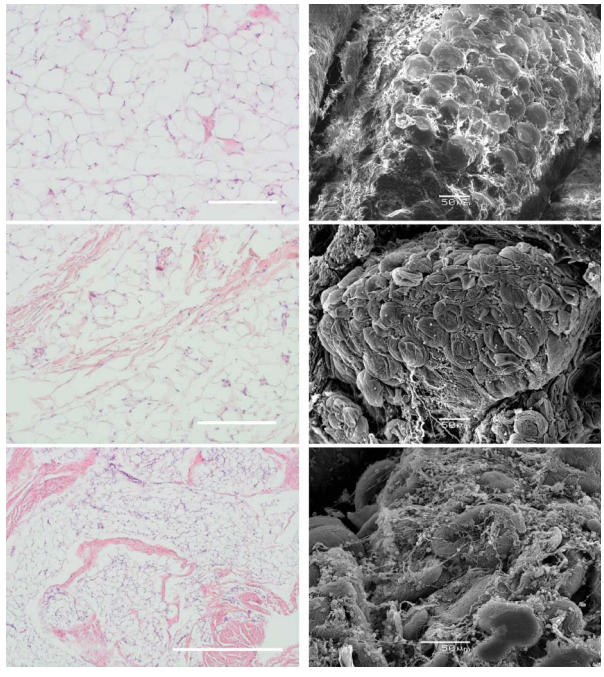

Figure 3. Light microscopy and SEM findings side by side: control/baseline (up, bar = 100 μm), 4 days (mid, bar = 200 μm), and 2 weeks (down, bar = 500 μm). Changes of fat tissue include delaminated membranes of adipocytes, alternations of their shape, presence of pyknotic nuclei, and subtle immune response, which started by day 4 and further propagated at 2 weeks. Conformational changes of collagen fibers were seen by day 4. SEM, scanning electron microscopy.

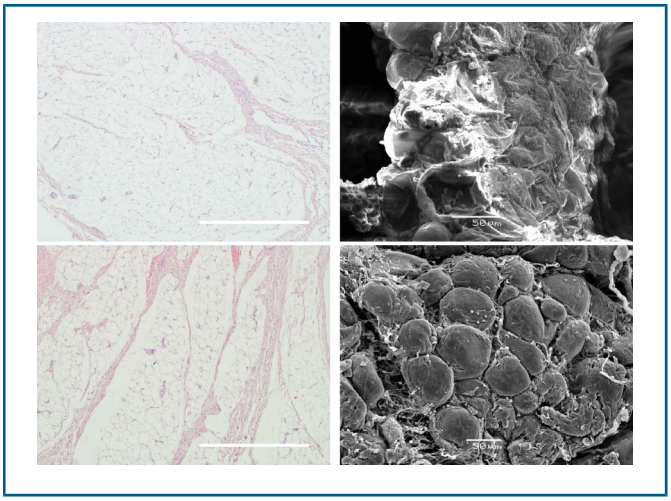

Figure 4. Light microscopy and SEM findings side by side at 1 month (up) and 2 months (down). At 1 month, the adipocytes still show membrane ruptures and alternations of their shape; however, the immune infiltrate is receding. At 2 months, the adipose tissue regenerates and is consisted of healthy-looking fat cells of smaller diameter. The architecture of interlobular septa was noticeably improved. SEM, scanning electron microscopy.

considerable decrease of adipocytes' area with the greatest reduction observed at 4 days (−25.9%; −337.8 μm^2) and 2 weeks (−31.1%; −405.5 μm^2) after the last procedure, when the most prominent changes in fat tissue were observed. Notably, the size of the adipocytes remained smaller at 1-month and 2-month follow-up compared with the baseline.

Scanning Electron Microscopy

Scanning electron microscopy micrographs corroborate the histology findings (Figures 3 and 4). At baseline, once again, healthy fat cells with well-defined shapes were observed. At the same time, 4 days after the last treatment, the adipocytes shrunk by 30% because of lipolysis with noticeable signs of membrane rupture. Fat cell elimination was more pronounced at 2 weeks with clearly visible lipolysis and the apoptotic events (Figure 3). A large number of disrupted adipocytes with extrusion of lipid droplets outside the ruptured and damaged cells were observed. A mild inflammatory infiltrate was present, indicating a local response to remove adipocyte cell remains.[20,21]

At 1 month, SEM micrographs showed that the adipose tissue still contained some damaged adipocytes, which had not yet been cleared (Figure 4). Surviving adipocytes were smaller because of lipolysis but showed signs of recovery and restoration of cell shape. Finally, 2 months after treatments, volume-depleted surviving adipocytes were almost back to baseline, although they still occasionally showed shape alternations (Figure 4).

Discussion

The histological and SEM evaluation of fat tissue after the dual RF/HIFEM treatment showed a corresponding pattern. Both H&E and SEM demonstrated lipolysis and a decrease in fat cells predicted to be long-term. Treatment effects in fat tissue peaked between 2 weeks and 1-month posttreatment when the most significant changes were seen. At 2 months, fat tissue still showed a significant and sustained fat reduction.

To accomplish a therapeutic effect in adipose tissue, it is necessary to achieve heating in a narrow range of 42 to 45°C, which triggers alternations in the structural integrity of the fat cells.[2,15] As shown in Figure 2, the lower limit of this temperature range was already achieved during the first 4 minutes. Temperature was then maintained within this range for the rest of the treatment. Such a rapid increase followed by a steady temperature profile allows for high efficiency because the therapeutic effect is delivered for 26 minutes of 30. This temperature profile is believed to be attributed to more uniform distribution of RF-generated heat, which is augmented by concomitant muscle activity and augmented blood circulation.[24] This hypothetically eliminates hot spots and contributes to treatment efficacy.

Previous studies have shown that controlled RF heating used as a standalone modality induces apoptosis.[20,21] Because only a mild inflammation response was observed, we believe

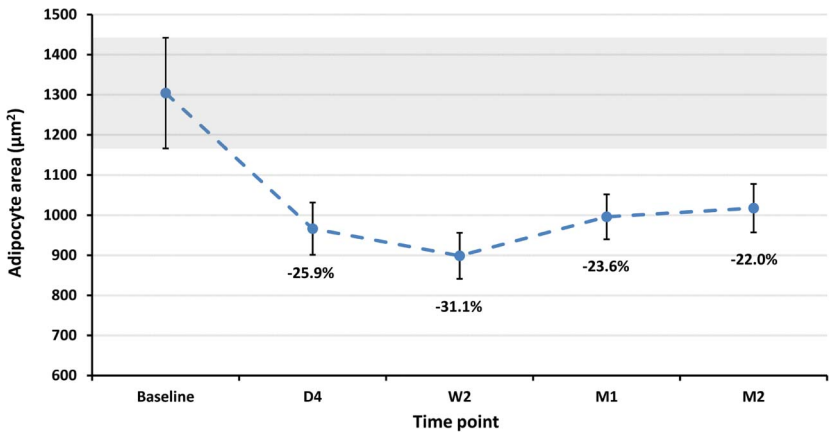

Figure 5. Average adipocyte area (mean ± standard error; μm^2) during the study. The decrease was highly statistically significant ($p < .001$) at all time points. The range for control and baseline samples is highlighted in gray.

that heat-induced necrosis was not the primary effect. This study shows that apoptosis is the more predominant mechanism than necrosis, with treated adipocytes showing pyknotic nuclei, delaminated membranes, shape alternations, and only a mild inflammatory response. Adipocytes also suffer apoptosis when their size significantly fluctuates while becoming too large or too small[11,26] and are stressed by the excessive efflux of FFAs.[13,27] Although RF is assumed to play a major role in the effect on fat tissue, HIFEM-induced lipolysis may augment the overall fat cell shrinkage and thus enhance the apoptotic effect of the RF treatment.

We believe that the very significant lipolysis observed in this study reflects simultaneous use of both modalities. First, RF heats the tissue and activates the sympathetic branch of the autonomic nervous system. This leads to the release of catecholamines (adrenaline and noradrenaline), which triggers lipolysis.[5] The magnetic field simultaneously applied leads to intense muscle contractions that requires considerable amount of energy. This additional energy demand is believed to stress adipocytes to deliver more by increasing metabolic pathways such as breakdown of triglycerides. More triglycerides are broken to FFAs, which are delivered through the circulation to the muscle tissue for β-oxidation and ATP production.[28]

Although RF heating alone induces lipolysis, some of the released FFAs may be a subject to lipogenesis if not consumed for energy, which may occur in all noninvasive fat reduction modalities.[26] The results from our study showed a sustained reduction of fat cells' size after 2 months, indicating that lipolysis was predominant. A major role in long-term fat reduction is extensive apoptosis. Our study shows extensive fat cell disruption by apoptosis in histological and SEM images.

In safety, neither RF (when used within safe parameters) nor HIFEM injures the skin, blood vessels, or other adjacent structures when used as a standalone modality for noninvasive body shaping.[3,5,8,11,13,20,23,27,29] This porcine study corroborates this finding with additional effects of better organization of interlobular septa with RF-induced activation of fibroblasts and subsequent collagen remodeling.[25,30] This study objectively shows effects of novel simultaneous synchronized RF and HIFEM technologies for porcine subcutaneous fat reduction. Limitations include whether this animal study will reflect results in human, although previous studies have shown that results in porcine models often reflect the results in human fat tissue.[31,32]

Conclusion

Simultaneous delivery of synchronized RF and high-intensity focused electromagnetic procedure demonstrated an excellent safety profile with no adverse events documented after 3 weekly treatments in a porcine model. Histology and SEM examination of adipose tissue revealed strong evidence of elimination of adipocytes through an apoptotic mechanism accompanied by a lipolytic effect, resulting in an overall fat tissue reduction. Induced changes were observed to peak during the first month, whereas at 2 months, a significant reduction of fat tissue was observed.

References

1. The American Society for Aesthetic Plastic Surgery. 2018 procedural statistics. Available from: https://www.surgery.org/media/statistics. Accessed January 2020.
2. Goats GC. Continuous short-wave (radio-frequency) diathermy. *Br J Sports Med* 1989;23:123–7.
3. Trelles MA, van der Lugt C, Mordon S, Ribé A, et al. Histological findings in adipocytes when cellulite is treated with a variable-emission radiofrequency system. *Lasers Med Sci* 2010;25:191–5.
4. Tanaka Y, Tsunemi Y, Kawashima M, Tatewaki N, et al. Treatment of skin laxity using multisource, phase-controlled radiofrequency in asians: visualized 3-dimensional skin tightening results and increase in elastin density shown through histologic investigation. *Dermatol Surg* 2014;40:756–62.
5. Vale AL, Pereira AS, Morais A, Noites A, et al. Effects of radiofrequency on adipose tissue: a systematic review with meta-analysis. *J Cosmet Dermatol* 2018;17:703–11.
6. Emilia del Pino M, Rosado RH, Azuela A, Graciela Guzmán M, et al. Effect of controlled volumetric tissue heating with radiofrequency on cellulite and the subcutaneous tissue of the buttocks and thighs. *J Drugs Dermatol* 2006;5:714–22.
7. Trelles MA, Mordon SR. Adipocyte membrane lysis observed after cellulite treatment is performed with radiofrequency. *Aesthet Plast Surg* 2009;33:125–8.
8. Weiss RA. Noninvasive radio frequency for skin tightening and body contouring. *Semin Cutan Med Surg* 2013;32:9–17.
9. Roth BJ, Basser PJ. A model of the stimulation of a nerve fiber by electromagnetic induction. *IEEE Trans Biomed Eng* 1990;37:588–97.
10. Duncan D, Dinev I. Noninvasive induction of muscle fiber hypertrophy and hyperplasia: effects of high-intensity focused electromagnetic field evaluated in an in-vivo porcine model: a pilot study. *Aesthet Surg J* 2020;40:568–74.
11. Duncan DI, Kim THM, Temaat R. A prospective study analyzing the application of radiofrequency energy and high-voltage, ultrashort pulse duration electrical fields on the quantitative reduction of adipose tissue. *J Cosmet Laser Ther* 2016;18:257–67.
12. Kinney BM, Kanakov D, Yonkova P. Histological examination of skin tissue in the porcine animal model after simultaneous and consecutive application of monopolar radiofrequency and targeted pressure energy. *J Cosmet Dermatol* 2020;19:93–101.
13. Halaas Y, Bernardy J. Mechanism of nonthermal induction of apoptosis by high-intensity focused electromagnetic procedure: biochemical investigation in a porcine model. *J Cosmet Dermatol* 2020;19:605–11.
14. Levi JR, Veerappan A, Chen B, Mirkov M, et al. Histologic evaluation of laser lipolysis comparing continuous wave vs pulsed lasers in an in vivo pig model. *Arch Facial Plast Surg* 2011;13:41–50.
15. Decorato JW, Chen B, Sierra R. Subcutaneous adipose tissue response to a non-invasive hyperthermic treatment using a 1,060 nm laser. *Lasers Surg Med* 2017;49:480–9.
16. Preciado JA, Allison JW. 59. The effect of cold exposure on adipocytes: examining a novel method for the non-invasive removal of fat. *Cryobiology* 2008;57:327.
17. Manstein D, Laubach H, Watanabe K, Farinelli W, et al. Selective cryolysis: a novel method of non-invasive fat removal. *Lasers Surg Med* 2008;40:595–604.
18. Chen GY, Nuñez G. Sterile inflammation: sensing and reacting to damage. *Nat Rev Immunol* 2010;10:826–37.
19. Rock KL, Kono H. The inflammatory response to cell death. *Annu Rev Pathol Mech Dis* 2008;3:99–126.
20. Boisnic S, Divaris M, Nelson AA, Gharavi NM, et al. A clinical and biological evaluation of a novel, noninvasive radiofrequency device for the long-term reduction of adipose tissue. *Lasers Surg Med* 2014;46:94–103.
21. McDaniel D, Fritz K, Machovcova A, Bernardy J. A focused monopolar radiofrequency causes apoptosis. *A Porcine Model* 2014;13:5.
22. Fenn AJ. *Breast Cancer Treatment by Focused Microwave Thermotherapy*. Oxfordshire, United Kingdom: Taylor & Francis, Jones & Bartlett Learning; 2007.

23. Adatto MA, Adatto-Neilson RM, Morren G. Reduction in adipose tissue volume using a new high-power radiofrequency technology combined with infrared light and mechanical manipulation for body contouring. *Lasers Med Sci* 2014;29:1627–31.
24. Joyner MJ, Casey DP. Regulation of increased blood flow (hyperemia) to muscles during exercise: a hierarchy of competing physiological needs. *Physiol Rev* 2015;95:549–601.
25. Meyer PF, de Oliveira P, Silva FKBA, da Costa ACS, et al. Radiofrequency treatment induces fibroblast growth factor 2 expression and subsequently promotes neocollagenesis and neoangiogenesis in the skin tissue. *Lasers Med Sci* 2017;32:1727–36.
26. Jo J, Shreif Z, Periwal V. Quantitative dynamics of adipose cells. *Adipocyte* 2012;1:80–8.
27. Weiss RA, Bernardy J. Induction of fat apoptosis by a non-thermal device: mechanism of action of non-invasive high-intensity electromagnetic technology in a porcine model. *Lasers Surg Med* 2019;51:47–53.
28. Lass A, Zimmermann R, Oberer M, Zechner R. Lipolysis—a highly regulated multi-enzyme complex mediates the catabolism of cellular fat stores. *Prog Lipid Res* 2011;50:14–27.
29. Pumprla J, Howorka K, Kolackova Z, Sovova E. Non-contact radiofrequency-induced reduction of subcutaneous abdominal fat correlates with initial cardiovascular autonomic balance and fat tissue hormones: safety analysis. *F1000Research* 2015;4:49.
30. Yokoyama Y, Akita H, Hasegawa S, Negishi K, et al. Histologic study of collagen and stem cells after radiofrequency treatment for aging skin. *Dermatol Surg* 2014;40:390–7.
31. Wang Q, Wang J, Wang T. Pigs can Be used as a large animal model for autologous fat grafting. *Ophthal Plast Reconstr Surg* 2016;32:73–4.
32. Houpt KA, Houpt TR, Pond WG. The pig as a model for the study of obesity and of control of food intake: a review. *Yale J Biol Med* 1979;52:307–29.

Received: 4 November 2020 | Revised: 22 January 2021 | Accepted: 26 January 2021

DOI: 10.1111/jocd.13970

ORIGINAL CONTRIBUTION

JCD Journal of Cosmetic Dermatology WILEY

Deletion of adipocytes induced by a novel device simultaneously delivering synchronized radiofrequency and hifem: Human histological study

David J. Goldberg MD, JD

Icahn School of Medicine, New York, NY, USA

Correspondence
David J. Goldberg MD, JD, Icahn School of Medicine, 110 E 55th St, New York, NY 10022, USA
Email: ddavidgoldberg@skinandlasers.com

Funding information
BTL Industries Inc., Grant/Award Number: This study was funded by a research grant

Abstract

Background: Radiofrequency (RF) is commonly recognized treatment option for fat reduction, utilizing heat-induced adipocyte deletion. HIFEM treatment has been proven to be an effective tool for body shaping.

Objectives: To document the structural changes in human subcutaneous tissue induced by the combination of RF treatment with the HIFEM procedure.

Methods: Four subjects (51.50 ± 6.35 years, 22.59 ± 3.21 kg/m^2) received three 30-minute abdominal treatments consisting of RF therapy and HIFEM. One subject (57 years, 23.60 kg/m^2) served as a control. Punch biopsies were collected at baseline, 1-week, and 1-month post-treatment. Samples were sliced and stained with H&E. Waist circumference, digital photographs, satisfaction, and therapy comfort were assessed. Subjects were monitored for any adverse event, and fat temperatures were measured.

Results: Baseline samples showed a healthy appearance of adipocytes, composed of round-shaped unilocular cells of uniform size. At follow-up, treated adipocytes demonstrated nuclear and shape changes with consequent fat reduction. Adipocytes were found to be flattened/shrunken and of smaller size (−33.5% at 1 week; −31.7% at 1-month) along with occasional ruptures of the cytoplasmic membrane. In contrast to baseline, pyknotic nuclei with condensed nuclear chromatin were seen at 1-week and 1-month post-treatment. The control samples showed no treatment-related changes. Waist circumference decreased by an average of 2.20 cm in the treated patients. No adverse events were observed. The fat temperature reached 42-45°C, during treatment; the therapy was comfortable with high patient satisfaction.

Conclusions: Results suggest the efficacy and safety of the therapy combining RF and HIFEM. The adipocyte deletion and shrinkage resulted in overall reduction of fat tissue.

KEYWORDS
apoptosis, HIFEM, histology, radiofrequency

1 | INTRODUCTION

Human subcutaneous fat tissue has a layered structure primarily consisting of fine collagen fibrous septa meshed with clusters of round-shape cells termed adipocytes.[1] Their cytoplasm is occupied by a large single lipid droplet, which serves as an energy reservoir, and is responsible for adipocytes spherical shape. Based on the amount of stored lipids, the adipocyte volume fluctuates throughout their lifetime.[2,3]

The continuous imbalance of caloric intake leads to the gradual accumulation of the adipose tissue since the excessive energy, which is not utilized by the body, is being stored in the lipid droplet in the form of triglyceride content.[2,3] A sedentary lifestyle and an unbalanced diet are considered the main contributors to increased fat storages in healthy human.[4] Besides the health risks and a need of considerable medical attention that often arise in the case of an overweight body,[5] the social aspects of a patient's well-being should not be underestimated as well. Aesthetically displeasing localized fat deposits are distressful for many and may result in the loss of self-esteem or trauma from embarrassment. Therefore, noninvasive body contouring has received increased attention in the recent years as a convenient solution for improving body image.

Noninvasive fat tissue reduction is energy-dependent and may be achieved either by reducing the fat stores or permanently removing adipocytes.[2] The first effect occurs when adipocytes are appropriately stimulated with energies of lower intensities, such as during low-level laser therapy (LLLT).[6] The catabolic process referred to as lipolysis is initiated, leading to a breakdown of the triglycerides stored in fat vacuoles into glycerol and free fatty acids (FFA) released into the vasculature.[7,8] However, although the decrease in adipocytes volume may be achieved by lipolysis, the cells are still viable and present in the same amount as before the therapy.

In addition to lipolysis, the adipose tissue can be eliminated permanently via various regulated cell death programs such as pyroptosis, necroptosis, and apoptosis.[9] Apoptosis is a complex intracellular pathway that allows the organism to control cell number and tissue size.[3,10] Morphologically, the most distinctive signs of apoptotic processes are cell shrinkage accompanied by nuclear changes in the form of chromatin condensation (pyknosis) and nuclear fragmentation (karyorrhexis).[2,11] Also, late plasma membrane disintegration may occur in case of extrinsic pathway of apoptosis.[9] Consequently, the cell remnants are digested by the immune cells during a phagocytic clearance.[12]

A specific amount of energy transformed into heat is required to induce fat apoptosis, elevating fat temperatures to 42-45°C. At the same time, it is necessary not to exceed the upper limit of 45°C in the long-term to avoid a risk of necrosis.[1,13-15] To safely heat the adipose tissue, various devices and technologies utilizing radiofrequency (RF) energy for fat apoptosis have been developed.[13,14,16,17] Due to the extensive research in the recent past, there exists a clear association between RF heating and adipocyte apoptosis documented in vivo in humans,[17] and correspondingly in porcine animal model.[14]

Nonetheless, body contouring may also be achieved via a nonthermal manner due to the muscle toning delivered by a high-intensity focused electromagnetic field (HIFEM) procedure.[18-20] HIFEM utilizes strong alternating magnetic fields, and based on the law of electromagnetic induction, it induces electric currents that depolarize neuromuscular tissue causing supramaximal muscle contractions. Such contractions demand a considerable amount of energy that is supplied in the form of FFA from adipose tissue via lipolysis.

The different modus operandi of the thermal (RF) and nonthermal (HIFEM) body contouring technologies allows for its combined use. An assumption arises that RF-induced fat loss may even be further promoted by the metabolic effect of HIFEM on fat when used simultaneously. Therefore, this study aims to document structural changes in human subcutaneous tissue induced by a novel device utilizing the simultaneous delivery of synchronized radiofrequency and HIFEM energy.

2 | MATERIALS AND METHODS

This was a prospective single-center study. Inclusion criteria were specified as BMI < 35.0 kg/m^2, no pregnancy or breastfeeding, injury in the treated area, active participation in any other concurrent therapy, and general contraindications for HIFEM and RF application to the human body. Five subjects were enrolled while four subjects (51.50 ± 6.35 years; BMI of 22.59 ± 3.21 kg/m^2) were assigned for active treatments, and one subject served as a control (57 years; BMI of 23.60 kg/m^2). At the time of enrollment, all study subjects were instructed about the study and associated procedures in detail. Written informed consent was obtained from all participants, and the study adhered to the ethical principles for medical research involving human subjects (1975 Declaration of Helsinki).

In total, the participants received three 30-minute abdominal treatments with a frequency of 1 treatment per week. No anesthesia or pretreatment, preparation was needed for the procedure. A device (Emsculpt NEO, BTL Industries INC., Boston MA) simultaneously delivering synchronized RF and HIFEM energies were used in this study. It utilizes a novel interspaced design of RF electrode that allows emitting radiofrequency and HIFEM fields in a synchronized manner, meaning that the apparatus for delivering both energies is embedded in one single applicator. Based on the patient's physical constitution, one or two applicators were placed over the treated area and affixed by an elastic fixation belt. The output power of RF was set to 100% in the active treatments and 5% for sham treatments. The intensity of HIFEM (0%-100%) in active group was cautiously adjusted according to the patient's feedback, ending up at a maximum tolerable level. HIFEM intensity in sham treatments was again set to 5%.

Punch biopsies (4 mm in diameter) of adipose tissue, after 1% lidocaine local anesthesia, were obtained from each subject at baseline, 1 week after the last treatment, and at 1-month follow-up. The baseline samples were collected at least 5 cm away from the

treatment site to avoid bleeding in the treated area and minimize patient discomfort during the therapy. Three tissue samples were collected from each subject (15 samples total). All specimens were preserved in a fixation solution (phosphate-buffered formalin), dehydrated, cleared, embedded in paraffin wax, and sectioned into thin (6 μm) slices using a microtome (120 micrographs in total). The slices were stained by the hematoxylin and eosin to finalize the processing for examination under the light microscope (Leica DM1000; Leica Microsystems, Germany). To evaluate structural changes of fat tissue, slices were subjected to detailed analysis by a certified histopathologist. The area of adipocytes (μm^2) in the examined slices was measured using Leica Application Suite Core Software and statistically analyzed by a two-tailed paired t test with $\alpha = 5\%$.

To verify the temperature distribution in the subcutaneous layer, the direct temperature measurements were taken using a flexible optic probe (LumaSense Technologies Inc, Germany) in one subject from the active group. Ultrasound-guided insertion of the probe into mid-depth of subcutaneous tissue was performed, and the temperature changes were monitored during the whole 30-minute treatment period.

Aside from histology, the secondary outcomes included documentation of treatment area by digital photographs, waist circumference, weight measurements, 5-point Likert scale satisfaction questionnaire, and 10-point visual analog scale (VAS) therapy comfort questionnaire assessed at baseline, 1-week, and 1-month follow-up. Any occurrence of adverse events was monitored throughout the study.

3 | RESULTS

All subjects successfully finished their treatments and follow-up visits. There were no adverse events reported. The only documented side effects were transient muscle soreness the day after the therapy and erythema that resolved within a few hours. Subjects rated their therapy comfort very high with average scores of 0.83 (active) and 0 (sham) at 10-point VAS (0 = no discomfort, 10 = unbearable discomfort).

Histological examination of baseline and control samples revealed healthy unilocular cells of round/polygonal shape. There were no deviations from the usual structure of adipose tissue (see Figure 1). On the contrary, the samples of treated tissue taken at 1 week showed visible shape alternations of fat cells and occasional fat ruptures. The evidence of ongoing programmed cell death processed was documented by the presence of pyknotic nuclei manifested by hypercondensation of chromatin and destructive fragmentation of the nucleus (Figure 2). Those findings persisted up to 1 month since the fat tissue still demonstrated an elevated level of adipocyte deletion and structural changes manifested as the flattening and plasma membrane disintegration (Figure 3). No such changes were found after the administration of sham treatment. Furthermore, no signs of necrosis were present after the active or sham treatments.

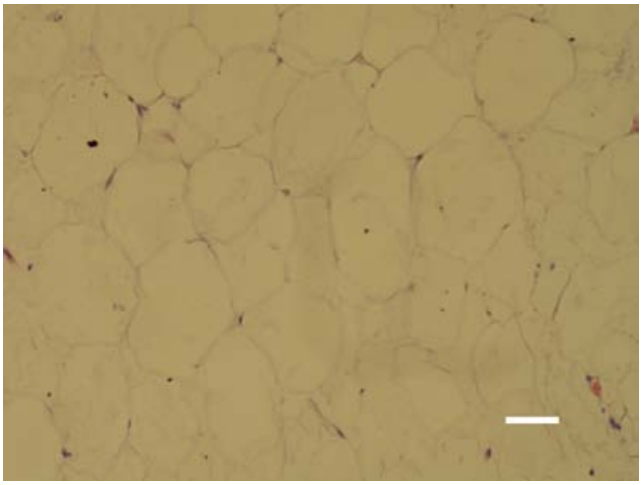

FIGURE 1 Subcutaneous tissue at baseline is consisted of healthy unilocular cells of round/polygonal shape (bar = 40 μm)

The outcomes of adipocyte size measurements can be seen in Figure 4. The fat cells in control samples were of a uniform size (approximately 1750 μm^2) throughout the study. The baseline measurements in the active group showed similar values, as seen in the control subjects. However, post-treatment samples showed a significant reduction in the adipocyte's size. At 1-week follow-up, the reduction in active group was 33.5% (−583 μm^2; $P = .009$), which was sustained at 31.7% (−552 μm^2; $P = .01$) at 1 month post-treatment. The loss of adipocytes content followed by its shrinkage/flattening was also apparent in examined histological samples. See Figures 2 and 3.

Fiber optic probe measurements showed a rapid increase in fat temperature in the first four minutes when the level of 42°C was achieved. The steady temperature range of 43-45°C was maintained for most of the therapy. In summary, the effective temperature needed to induce structural changes in adipose tissue was held most of the treatment time (Figure 5).

Weight fluctuations in the active group were insignificant (−0.2 kg at 1 week and −0.3 kg at 1 month, respectively). The changes in fat tissue observed by the microscopic evaluation were projected into a visible improvement of abdominal body contour (see Figure 6). The average waist circumference reduction in the active group was −2.20 cm with a maximum 5.4 cm reduction. Concurrently, the control subject showed no improvement in waist circumference. Active treatment resulted in a much greater satisfaction rate with therapy outcomes. Patients who received therapy with maximum intensities agreed (4) or strongly agreed (5) with the statement that the appearance of their abdominal area improved while the sham subject disagreed (2).

4 | DISCUSSION

The study investigated the effects of a novel technology utilizing simultaneous delivery of synchronized radiofrequency heating and

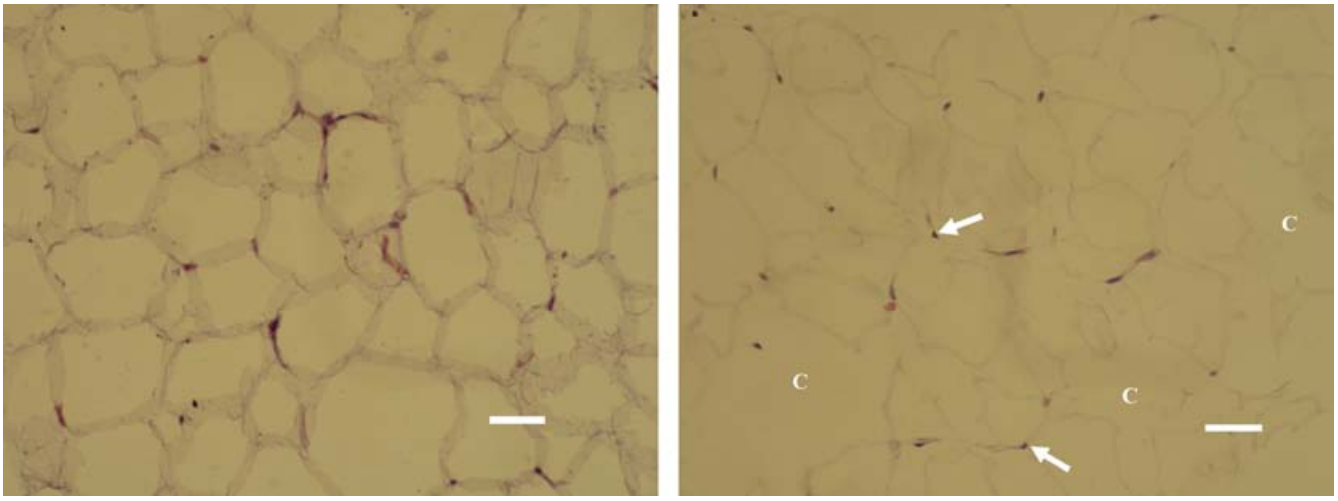

FIGURE 2 Elimination of fat cells (C), noticeable shape alternations, and pyknotic nuclei (depicted by an arrow) found in the treated adipose tissue at 1 wk (right, bar = 30 μm). No changes were found in control/sham subject (left, bar = 30 μm)

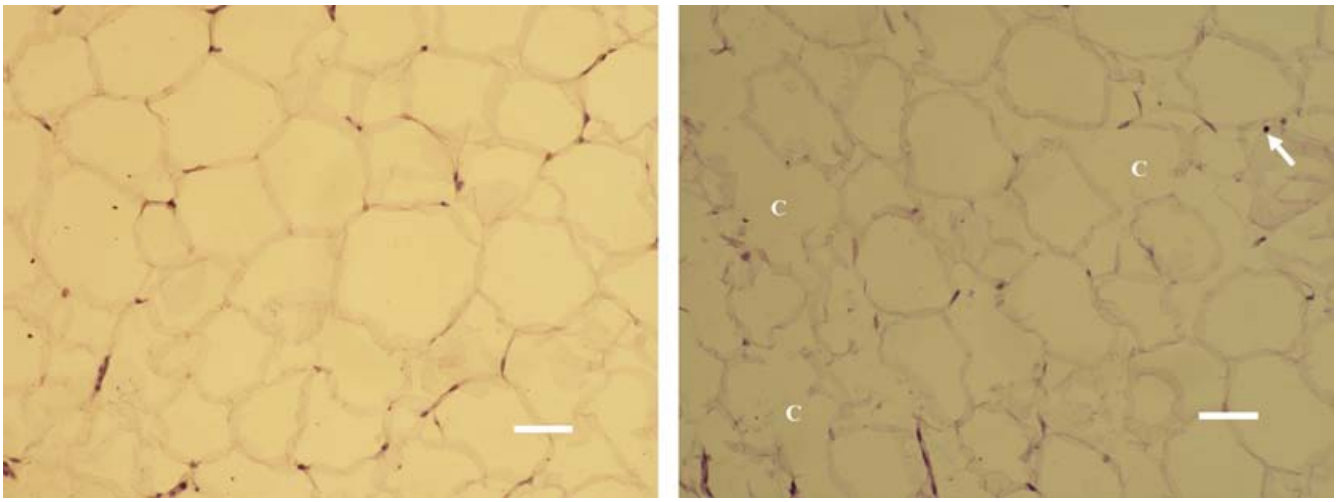

FIGURE 3 Elimination of fat cells (C), pyknotic nuclei (arrow), and shrinkage of adipocytes were found at 1 mo in treated subjects (right, bar = 30 μm). No changes were present after the sham treatment (left, bar = 30 μm)

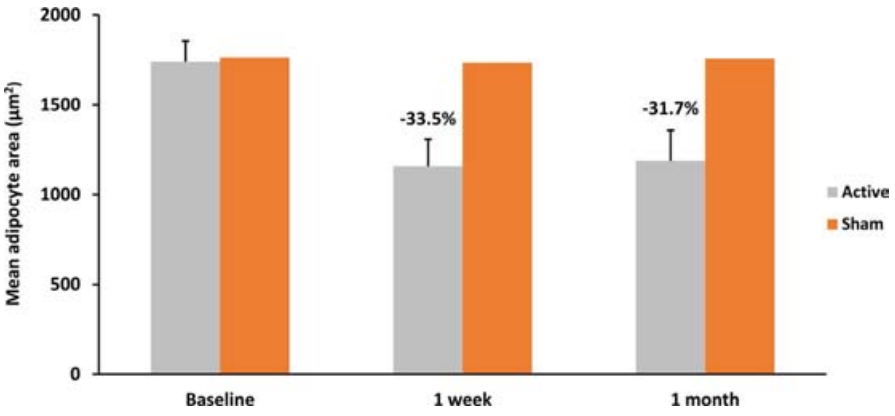

FIGURE 4 Adipocytes showed a significant ($P < .05$) decrease in size after the active treatment compared with sham at 1 wk and 1 mo. The error bars represent the variability of results among the subjects

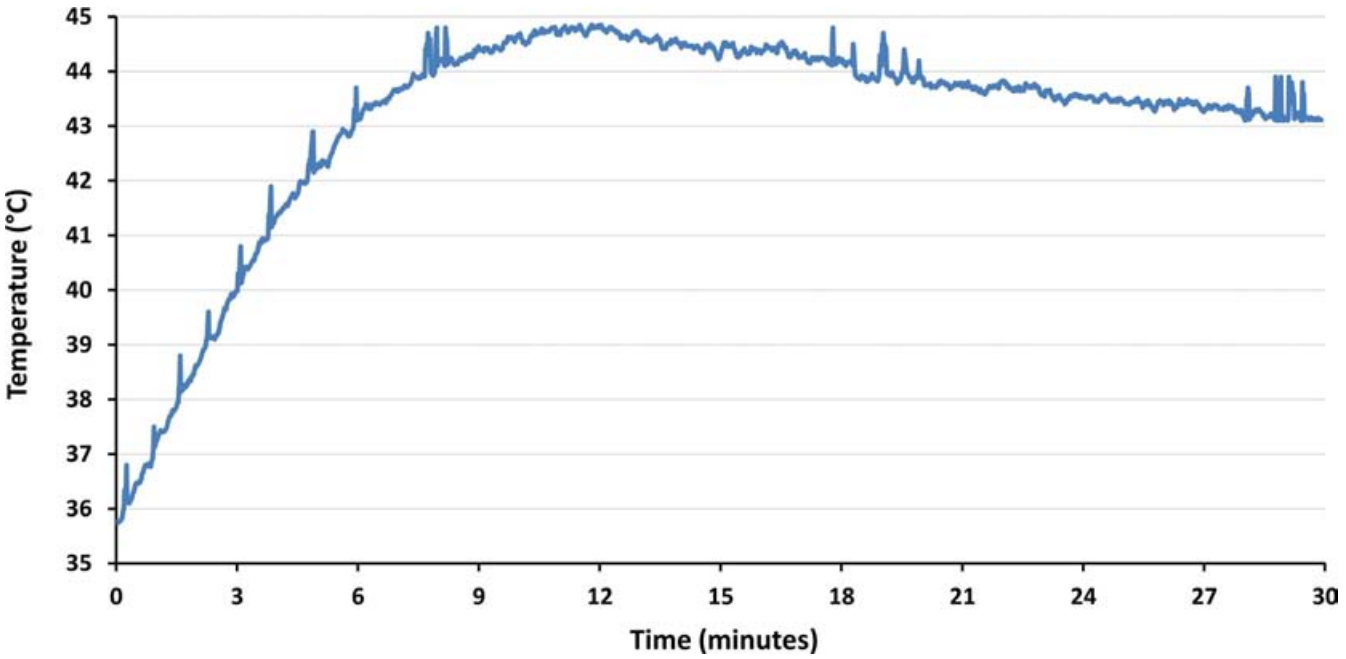

FIGURE 5 Rapid increase in fat temperature was seen, exceeding 42°C after the fourth minute. For most of the therapy time, the temperature was maintained at the level needed to induce structural changes to adipose tissue

FIGURE 6 Illustration of treatment outcomes by digital photographs (57 y, 22.98 kg/m^2). There is a noticeable improvement of the abdominal body contour seen at 1 mo (right) compared with baseline (left)

HIFEM stimulation on subcutaneous adipose tissue. Histological evaluation based on H&E staining showed prominent alterations within the adipose tissue at 1 week and 1 month post-treatment in subjects who received active treatment. No changes in the tissue were seen in the sham patient.

The results indicate that the simultaneous treatment triggers lipolysis along with fat cell elimination. The reduced adipocyte size is strong evidence for lipolysis as the adipocytes lose their intracellular content due to the breakdown of triglycerides into glycerol and FFA, which are subsequently liberated into the blood stream. The intracellular content has been reduced by 33.5% at 1 week and by 31.7% at 1 month compared with baseline. Also, the mean cross-sectional area at both follow-ups shows relatively small variation (see Figure 4), indicating that decrease in adipocytes size was uniform across all cells rather than it was a matter of some extreme values or outliers. Supposedly, the lipolytic effect of the simultaneous treatment may be attributed to both modalities, HIFEM and RF, as radiofrequency heating is known to trigger the lipolysis, and the supramaximal contractions induced by HIFEM were documented to result in increased metabolic activity, also leading to the fat lipolysis.[21]

Regarding adipocyte deletion, the presence of pyknotic nuclei, alternations of adipocytes shape, and absence of the inflammation are strong indicators of apoptotic changes happening in the tissue, since the pyknosis is irreversible and leads to nuclear fragmentation and cell death. Thus, the increased presence of pyknotic nuclei suggests elevated number of cells that entered the apoptotic process. This is also supported by the temperature measurements which

have shown that the temperature in the fat tissue reaches 42°C after 4 minutes and remains between 43 and 45°C during the most of the treatment, effectively triggering the adipocyte apoptosis.[16] On the other hand, although the observed plasma membrane disintegration might be a consequence of apoptotic-related decomposition, it also may indicate the presence of distinct regulated cell death pathways like pyroptosis.[9] However, the examination of the fat tissue at molecular level needs to prove this hypothesis which is beyond the scope of this study.

The efficacy of the simultaneous application of HIFEM and synchronized RF seen herein is in agreement with previous research that has shown a 29.8% reduction in the subcutaneous fat layer, as measured by ultrasound imaging system, and similar histological changes as seen in this study.[22] Future research can be used to look at programmed cell death markers for adipocytes[9,23] as well as to determine the duration of induced changes in a broader patient sample.

Individuals willing to improve their abdominal body contour may benefit from a mutual combination of the synchronized RF and HIFEM energies. This study documents that the simultaneous use of both investigated technologies is safe and results in noticeable body shaping effect, achieved primarily by the reduction in size and numbers of fat cells.

CONFLICT OF INTEREST

This study was funded by a research grant from BTL Industries Inc.

DATA AVAILABILITY STATEMENT

The data that support the findings of this study are available from the corresponding author upon reasonable request.

ORCID

David J. Goldberg https://orcid.org/0000-0002-8950-439X

REFERENCES

1. Jimenez Lozano JN, Vacas-Jacques P, Anderson RR, Franco W. Effect of Fibrous Septa in Radiofrequency Heating of Cutaneous and Subcutaneous Tissues: Computational Study: EFFECT OF FIBROUS SEPTA IN RF HEATING. *Lasers Surg Med*. 2013;45(5):326-338.
2. Sorisky A, Magun R, Gagnon A. Adipose cell apoptosis: death in the energy depot. *Int J Obes*. 2000;24(S4):S3-S7.
3. Prins JB, Walker NI, Winterford CM, Cameron DP. Apoptosis of Human Adipocytes in Vitro. *Biochem Biophys Res Commun*. 1994;201(2):500-507.
4. Jebb SA, Moore MS. Contribution of a sedentary lifestyle and inactivity to the etiology of overweight and obesity: current evidence and research issues. *Med Sci Sports Exerc*. 1999;31(Supplement 1):S534.
5. Field AE, Coakley EH, Must A, et al. Impact of Overweight on the Risk of Developing Common Chronic Diseases During a 10-Year Period. *Arch Intern Med*. 2001;161(13):1581.
6. Caruso-Davis MK, Guillot TS, Podichetty VK, et al. Efficacy of low-level laser therapy for body contouring and spot fat reduction. *Obes Surg*. 2011;21(6):722-729.
7. Duncan RE, Ahmadian M, Jaworski K, Sarkadi-Nagy E, Sul HS. Regulation of lipolysis in adipocytes. *Annu Rev Nutr*. 2007;27:79-101.
8. Langin D. Adipose tissue lipolysis as a metabolic pathway to define pharmacological strategies against obesity and the metabolic syndrome. *Pharmacol Res*. 2006;53(6):482-491.
9. Zhang Y, Chen X, Gueydan C, Han J. Plasma membrane changes during programmed cell deaths. *Cell Res*. 2018;28(1):9-21.
10. Jeyakumar SM, Vajreswari A, Sesikeran B, Giridharan NV. Vitamin A supplementation induces adipose tissue loss through apoptosis in lean but not in obese rats of the WNIN/Ob strain. *J Mol Endocrinol*. 2005;35(2):391-398.
11. Xu X, Lai Y, Hua Z-C. Apoptosis and apoptotic body: disease message and therapeutic target potentials. *Biosci Rep*. 2019;39(1):BSR20180992.
12. Erwig L-P, Henson PM. Clearance of apoptotic cells by phagocytes. *Cell Death Differ*. 2008;15(2):243-250.
13. Boisnic S, Divaris M, Nelson AA, Gharavi NM, Lask GP. A clinical and biological evaluation of a novel, noninvasive radiofrequency device for the long-term reduction of adipose tissue. *Lasers Surg Med*. 2014;46(2):94-103.
14. McDaniel D, Fritz K, Machovcova A, Bernardy J. A focused monopolar radiofrequency causes apoptosis: a porcine model. *J Drugs Dermatol*. 2014;13(11):1336-1340.
15. Fenn AJ. *Breast Cancer Treatment by Focused Microwave Thermotherapy*. Burlington, MA: Jones & Bartlett Learning; 2007.
16. Franco W, Kothare A, Ronan SJ, Grekin RC, McCalmont TH. Hyperthermic injury to adipocyte cells by selective heating of subcutaneous fat with a novel radiofrequency device: Feasibility studies. *Lasers Surg Med*. 2010;42(5):361-370.
17. McDaniel D, Lozanova P. Human adipocyte apoptosis immediately following high frequency focused field radio frequency: case study. *J Drugs Dermatol*. 2015;14(6):622-623.
18. Kent DE, Jacob CI. Simultaneous Changes in Abdominal Adipose and Muscle Tissues Following Treatments by High-Intensity Focused Electromagnetic (HIFEM) Technology-Based Device: Computed Tomography Evaluation. *J Drugs Dermatol*. 2019;18(11):1098-1102.
19. Kinney BM, Lozanova P. High intensity focused electromagnetic therapy evaluated by magnetic resonance imaging: Safety and efficacy study of a dual tissue effect based non-invasive abdominal body shaping: MRI EVALUATION OF ELECTROMAGNETIC THERAPY. *Lasers Surg Med*. 2019;51:40-46.
20. Kinney BM, Kent DE. MRI and CT Assessment of Abdominal Tissue Composition in Patients After High-Intensity Focused Electromagnetic Therapy Treatments: One-Year Follow-Up. *Aesthet Surg J*. 2020;40:NP686-NP693.
21. Halaas Y, Bernardy J. Mechanism of nonthermal induction of apoptosis by high-intensity focused electromagnetic procedure: Biochemical investigation in a porcine model. *J Cosmet Dermatol*. 2020;19(3):605-611.
22. U.S. Food and Drug Administration. 510(k) Premarket Notification: K192224. Published online December 5, 2019. https://www.accessdata.fda.gov/cdrh_docs/pdf19/K192224.pdf. Accessed September 24, 2020.
23. Kosacka J, Koch K, Gericke M, et al. The polygenetically inherited metabolic syndrome of male WOKW rats is associated with enhanced autophagy in adipose tissue. *Diabetol Metab Syndr*. 2013;5(1):23.

How to cite this article: Goldberg DJ. Deletion of adipocytes induced by a novel device simultaneously delivering synchronized radiofrequency and hifem: Human histological study. *J Cosmet Dermatol*. 2021;00:1–6. https://doi.org/10.1111/jocd.13970

Efficacy and Safety of Simultaneous Application of HIFEM and Synchronized Radiofrequency for Abdominal Fat Reduction and Muscle Toning: A Multicenter Magnetic Resonance Imaging Evaluation Study

Carolyn Jacob, MD,* David Kent, MD,† and Omer Ibrahim, MD*

BACKGROUND Radiofrequency and high-Intensity Focused Electromagnetic (HIFEM) field procedure are well-known, stand-alone, body-shaping modalities, yet their simultaneous application has not been investigated.

OBJECTIVE The aim is to evaluate the efficacy of a novel device simultaneously delivering HIFEM and radiofrequency for subcutaneous fat reduction and muscle toning.

MATERIALS AND METHODS Forty-one subjects with an average age of 39.7 ± 11.5 years were recruited. The subjects received 3 abdominal treatments (one per week). Magnetic resonance imaging images of the treated area were evaluated at baseline and at 1-, 3-, and 6-month visits for changes in subcutaneous fat, muscle thickness, and abdominal separation (AS). Anthropometric data and digital photographs were collected. Subject satisfaction and therapy comfort were evaluated.

RESULTS The muscle mass increase peaked at 3 months, showing 26.1% thickening. The fat thickness reduction was most prominent at 3 months, showing a 30.8% reduction. The AS decreased by 18.8% at 3 months after treatment. The waist circumference reduced by 5.87 ± 3.64 cm at a 3-month follow-up. Six-month data showed maintenance of these outcomes. The treatment was considered as comfortable with high patient satisfaction.

CONCLUSION The analysis of magnetic resonance imaging images and waist measurements showed that the therapy combining HIFEM and radiofrequency is highly effective in reducing subcutaneous fat and muscle thickening.

The field of noninvasive body shaping is primarily represented by 2 types of devices.[1] The first type is focused on subcutaneous fat reduction through thermal stress, either heating or cooling, which induces damage to fat cells. These devices utilize cryolipolysis, radiofrequency (RF), focused ultrasound, or lasers to induce the thermal stress.[2]

The second approach in noninvasive body shaping is focused on muscular tissue. The first widely used device introduced only in 2018[3] is based on high-Intensity Focused Electromagnetic (HIFEM) technology, which generates an alternating magnetic fields that induce electric current in the tissue, which stimulates motor neurons and triggers muscle contractions. The therapy was found to result in a significant thickening of muscle tissue while having an effect on subcutaneous adipose tissue as well.[4–6]

However, to achieve the total body shaping effect, that is, fat reduction and toned muscles, a combination of these 2 modalities would be optimal. This approach is common, but it is time consuming for the patient and the practice because the devices can only be used consecutively. Therefore, a technology that simultaneously combines the muscle stimulation and fat reduction modalities would be highly beneficial.

The outcomes of recent research suggest that muscle stimulation and tissue heating could work in synergy and promote the effects on the muscles.[7–9] Goto and colleagues[10] showed that the simultaneous application of heat and mechanical stimulation to muscle induces significantly higher expression of heat shock proteins that play a crucial role in muscle hypertrophy by promoting muscle protein synthesis.[11] Similarly, both heat and mechanical stimuli can activate myosatellite cells—muscle-derived stem cells involved in myofiber development and renewal.[12]

Synergistic effects of the simultaneous application of heat and muscle stimulation could also manifest in the adipose tissue. Also, HIFEM-induced localized muscle workload increases the demand for energy and thus the fat metabolism.[4,5] Heat itself increases lipolysis, and when sustained at temperatures of 42 to 45°C, adipocytes lose their cellular integrity and undergo apoptosis.[13] Adipose tissue could thus be affected in 2 different ways, which may translate into boosting the treatment outcomes.

*From the *Chicago Cosmetic Surgery and Dermatology, Chicago, Illinois; †Skin Care Physicians of Georgia, Macon, Georgia*

The authors have indicated no significant interest with commercial supporters.

Address correspondence and reprint requests to: Carolyn Jacob, MD, 515N State St Ste 900, Chicago, IL 60654, or e-mail: cjacob@chicagodermatology.com

http://dx.doi.org/10.1097/DSS.0000000000003086

For such purpose, a novel technology allowing simultaneous application of HIFEM and RF in a synchronized manner has been developed. The technology overcomes the interferences between the 2 modalities by a unique design of synchronized RF electrodes that prevent the creation of eddy currents. It is hypothesized that the technology for the simultaneous application of HIFEM and synchronized RF should result in synergistic effects in both muscle and adipose tissues. Therefore, this study aims to investigate the efficacy and safety of such novel technology for abdominal body shaping.

Materials and Methods

Study Population

Forty-one subjects (17 men and 24 women) interested in the noninvasive aesthetic improvement of abdomen participated in this prospective, multicenter, open-label, single-arm study. The inclusion criteria included adult subjects of any gender with a body mass index (BMI) lower than 35 kg/m^2. The study's exclusion criteria were pregnancy, postpartum period, breastfeeding, injury in the treatment area, or any other medical conditions that contraindicate the application of electromagnetic fields and RF, such as cardiovascular disease, malignant tumor, metal, or electronic implants. Subjects who met the inclusion criteria and were recruited as study participants were, on average, 39.7 ± 11.5 years old and had a BMI of 26.56 ± 3.73 kg/m^2 at the beginning of the study.

Study Design

The study design and the treatment protocol were approved by the Institutional Review Board and followed the ethical guidelines of the 1975 Declaration of Helsinki.

Each subject received three 30-minute treatments on the abdomen with the device simultaneously delivering HIFEM and RF energies through a single applicator (Emsculpt NEO, BTL Industries, Inc., Boston, MA). The treatments were administered once a week. All of the patients were instructed to maintain their daily routine and not to change their lifestyle. Before the treatment, each subject received detailed instructions about the study and signed informed consent.

During the treatments, no anesthesia was required. Patients were positioned in a supine position with the applicators centered over the umbilicus. In case the patients' constitution allowed, 2 applicators were used bilaterally, centered above both lateral sides of the rectus abdominis. Applicators were affixed with a fixation belt to avoid the possibility of movement during the treatment. Each treatment lasted for 30 minutes, starting with the HIFEM intensity set to 0%, increasing it to the maximum tolerable level. The RF intensity was set to 100% since the beginning of the procedure. Patients were regularly asked about the therapy comfort during the whole treatment time, and the energy settings were adjusted accordingly. Digital photographs of the treatment area, waist circumference measurements, weight and height records, and magnetic resonance imaging (MRI) images of the treatment area were collected at baseline and at 1-, 3-, and 6-month follow-up visits.

Data Collection and Evaluation

Magnetic resonance imaging was used as the primary evaluation modality for assessing the treatment effects on muscle and adipose tissue thickness and abdominal separation (AS) width. The scanning area was defined by T12 and S1 vertebrae. The images were acquired by the FIESTA and FSPRG sequences (Matrix: 380 × 380, ST: 5 mm, Spacing: 1 mm) in a transverse plane. The muscle and fat thickness measurements were performed supraumbilically and infraumbilically, approximately 2 inches (5 cm) above and below the umbilicus. The AS was measured at the same MRI slices as a perpendicular distance between the 2 parallel pairs of rectus abdominis muscle. Data collection was done at baseline and at 1-, 3-, and 6-month follow-ups.

The patient's satisfaction with the treatment results was assessed using the Satisfaction Questionnaire with a 5-point Likert scale after the last treatment and each follow-up visit. The therapy comfort was evaluated using 10-point visual analogue scale (VAS) after each treatment session.

All data were statistically analyzed using repeated-measures analysis of variance, paired, and 2-sample *t*-test. Analyses showing *p*-values of $<.05$ were considered as significant.

Results

Forty patients completed the entire treatment procedure and attended the MRI screening at 1-month follow-up. One subject withdrew from the study before completing the whole procedure. Twenty-nine patients attended the 3-month follow-up visit, and 20 patients participated at the 6-month follow-up visit, including the MRI screening. The dropout rate seen at the MRI follow-up visits was considerably affected by the outbreak of COVID-19, which did not allow the patients to attend the visits in person. Therefore, 4 of these patients attended the 3- and 6-month follow-up visits virtually, where they were asked to report any adverse events, satisfaction with results, weight, and waist circumference measurements. These patients did not undergo MRI screening due to the restrictive measures.

Magnetic Resonance Imaging Evaluation

Subcutaneous Adipose Tissue

Evaluation of 1-month scans showed an average fat reduction across the abdomen by 24.4%. The patients lost 23.6% on average (−6.61 ± 2.9 mm) infraumbilically and 25.3% on average (−5.9 ± 2.7 mm) supraumbilically. The results were fairly consistent; although only 2 patients showed a reduction lower than 5%, 37 patients showed a reduction higher than 15%, and 33 patients showed a reduction higher than 20%.

At 3 months, the results further improved significantly ($n = 29$; $p < .05$) in comparison to 1 month as the patients lost, on average, 30.8% of fat since the baseline visit. Supraumbilically, the patients lost 7.3 ± 3.3 mm (31.9%) on average and 7.9 ± 2.5 mm (29.7%) infraumbilically. At 3-month follow-up, there were no nonresponders with

TABLE 1. Detailed Result Summary of MRI Measurements					
Measurement	**Location**	**Baseline (*N* = 40)**	**1M FU (*N* = 40)**	**3M FU (*N* = 29)**	**6 M FU (*N* = 20)**
Fat thickness	Infraumbilicus	28.6 ± 11.8 mm	22.0 ± 10.0 (−23.6%)	19.9 ± 8.1 (−29.7%)	21.0 ± 8.9 (29.1%)
	Supraumbilicus	24.2 ± 11.7 mm	18.3 ± 9.8 (−25.3%)	16.4 ± 8.5 (−31.9%)	17.8 ± 8.2 (27.5%)
Muscle thickness	Infraumbilicus	9.2 ± 2.3 mm	11.2 ± 2.5 (+22.0%)	11.6 ± 3.0 (+24.7%)	11.2 ± 2.2 (26.4%)
	Supraumbilicus	8.7 ± 2.3 mm	10.7 ± 2.5 (+24.9%)	11.1 ± 2.7 (+27.4%)	10.6 ± 2.0 (24.1%)
Abd. separation	Infraumbilicus	16.6 ± 6.3 mm	13.7 ± 5.6 (−17.8%)	12.9 ± 4.9 (−19.6%)	12.4 ± 5.3 (20.0%)
	Supraumbilicus	21.4 ± 6.3 mm	18.1 ± 5.5 (−15.8%)	17.4 ± 5.2 (−18.8%)	17.8 ± 5.3 (19.6%)

MRI, magnetic resonance imaging; FU, follow-up; M, month.

reduction lower than 5%. Twenty-eight out of the 29 patients showed a reduction higher than 20%, and in 23 patients, the reduction exceeded 25%. All changes were statistically significant ($p < .05$).

In the group of 20 subjects who underwent the MRI screening at 6-month follow-up showed that the improvement achieved at 3 months (30.8%) was mostly preserved with the average reduction of 28.3% in comparison to baseline, yet showing a statistically insignificant ($p > .05$) decreasing trend. At 6 months, 7 out of the 20 subjects showed a decrease in the improvement of more than 5% when compared with the results at 3-month follow-up.

Table 1 shows a detailed result summary. An example of a patient MRI scan can be seen in Figure 1.

Muscular Tissue

The thickness of the rectus abdominis was increased by 23.5% on average at 1-month posttreatment. At infraumbilical slices, the average increase was equal to 1.9 ± 0.7 mm in absolute values corresponding to an average 22.0% increase in the thickness. Supraumbilical slices showed thickening by 2.0 ± 0.8 mm, corresponding to 24.9% increase on average. There were no nonresponding patients, and in 32 out of 40 patients, the thickness of rectus abdominis increased by more than 18%.

Similar to the fat tissue, the results in muscles continued to improve at 3-month follow-up. The average increase in muscle thickness was 26.1% (+2.3 ± 0.8 mm), whereas 24.8% thickening was seen infraumbilically and 27.4% supraumbilically. All changes were statistically significant ($p < .05$).

At 6 months, the MRI scans of 20 subjects showed that the results of these patients were maintained. Data of this group showed a 25.8% thickening at 3 months, which was then maintained at 25.3% at 6-month follow-up visit.

Table 1 shows a detailed result summary.

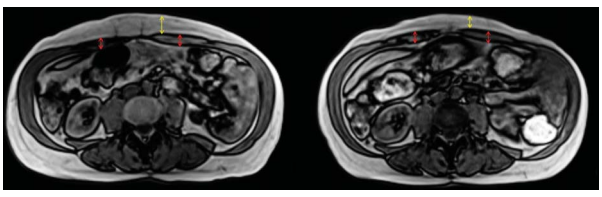

Figure 1. Magnetic resonance images illustrating the changes in the treated area. Supraumbilical slices taken at baseline (left) and at 3-month follow-up (right) of a 62-year-old woman. Individual patient's improvement reached −45.6% in fat reduction and +14.6% in muscle thickness, respectively. Fat tissue is marked with yellow arrows, rectus abdominis muscle by red color.

Abdominal Separation

The width of AS reduced significantly ($p < .05$) at both the supraumbilical and infraumbilical slices in all of the examined subjects. Supraumbilically, the average width of AS was reduced by 16.0% at 1-month follow-up and by 17.6% at 3-month follow-up. Infraumbilically, the AS reduced by 16.4% at 1 month and by 19.2% reduction at 3-month follow-up (detailed results are given in Table 1).

According to the supraumbilical slices, 8 out of the 40 patients experienced diastasis recti at baseline. It is a condition when the gap between the 2 sides of rectus abdominis muscles exceeds 27 mm.[14] In this group, the AS was reduced by 4.8 ± 1.7 from 30.1 ± 2.1 mm at baseline to 25.4 ± 2.0 mm at 1-month follow-up. In 6 patients, the condition was fully corrected at 1-month follow-up.

At 6 months, the overall reduction in AS was 19.8%. Of the 20 subjects examined at 6 months, 5 experienced diastasis recti at baseline. At 6 months, 4 subjects were fully without diastasis recti, and only a single subject exceeded the 27-mm range, yet this subject showed a prominent reduction as at baseline: the AS was 33.4 mm, whereas the 6-month measurements showed an AS of 27.5 mm.

Patient Satisfaction and Treatment Comfort

The patients found the treatments comfortable with a score of 2.3 ± 1.8 on a 10 point VAS (0 = no discomfort; 10 = unbearable pain). By the end of the first treatment, most patients reached 100% intensity of the HIFEM field. The intensity of RF was adjusted in most patients based on their individual perception of the heat.

The satisfaction questionnaire's analysis revealed high patient satisfaction as 91% of patients reported satisfaction

with the treatment results at 3-month posttreatment. Ninety-four percent of patients reported improved appearance of the abdomen, and 91% reported improvement in both muscle and fat.

No severe adverse events or side effects of the treatment were reported. In all patients, the treatment was associated with mild erythema following treatment and dissipated rapidly, and some patients experienced mild muscle soreness on the day after treatment.

Waist Circumference and Weight Measurements

The waist circumference was reduced by 3.3 ± 3.1 cm on average at 1-month follow-up visit. At 3 months, the average circumferential reduction was 5.9 ± 3.6 cm. The patients attending 6-month visit showed a 6.7 ± 3.5 cm reduction in waist circumference. The weight did not show any major fluctuations between any of the time points. Digital photographs showed notable improvement. Figure 2 provides an example of patients' result.

Discussion

The treatments with a novel device that delivers HIFEM and synchronized RF energies simultaneously resulted in a statistically significant increase in muscle mass, reduction in the fat layer thickness, and reduction in AS. The results in all 3 measured parameters showed improvement up to 3 months at which time the results peaked. The MRI observations were accompanied by reduced waist circumference and improved body image in digital photographs. At 6 months, no further improvements were observed, but the results seen at a 3-month follow-up were maintained in the majority of the patients. Although the results at 6 months are still highly above baseline values, the patients may benefit from additional maintenance treatments to reverse the declining tendency and to prolong the longevity of achieved outcomes.

The study did not include control groups that would receive HIFEM-only and RF-only treatments. However, several studies were published in the past solely for these modalities, allowing for comparison with the outcomes of this study. Studies on the abdominal application of HIFEM did show an average subcutaneous fat reduction[6,15,16] of 19.6% (17.5%–23.3%), average muscle thickening[6,15] of 15.1% (14.8%–15.4%), and an average reduction in AS[6,15] by 9.95%. When compared with our results with the simultaneous application of HIFEM and RF, it appears that the synergy of the 2 energies has a truly high impact on the final outcome because it yields more than 50% higher improvement in all 3 measured parameters.

Studies[13,17–21] investigating the application of RF systems for subcutaneous fat reduction report a fat thickness reduction ranging from 4.9% to 29.0% with a weighted average of 14.58%. Nevertheless, the comparison with other RF studies may not be as precise because the studies investigate various systems of different frequencies and other properties. However, they do provide an overview of the expected patient results of treatment with this modality.

Our results are in agreement with the fact that combination treatments in general are considered more effective than stand-alone treatments. Study by Kilmer and colleagues[22] found that consecutive treatments of cryolipolysis and electromagnetic technology result in better subjective perception of the treatment outcomes than stand-alone treatments as seen in patient satisfaction or photographic evaluation. The study also reported higher waist circumference reduction after the combined treatments of 1.5 cm. Considering this result, it can be seen that simultaneous application of HIFEM and RF is more effective in waist reduction (−5.9 cm) than consecutive application of cryolipolysis and electromagnetic technology (−1.5 cm).

Although this is a first MRI study investigating the effects of simultaneous application and further research is necessary to validate these findings, the results seem to exceed the outcomes of individual HIFEM and RF treatment. Regarding muscle tissue, it is assumed that the synergistic effect could be attributed to the physiologic nature of muscle synthesis regulating molecules, such as heat shock proteins[10] and satellite cells,[12] which concentrations and state can be altered by both mechanical stimulation and heat.

One of the study limitations is the high dropout rate at the 3- and 6-month follow-ups, mainly attributed to the outbreak of COVID-19, as attending follow-up visits would pose risks of infection to the patients. However, 29 patients out of 40 at a 3-month visit represent 72.5% of the initial population and still provide valuable data about the treatment outcomes. The lack of a control group can also be considered as a limitation and should be implemented in future studies.

Figure 2. Digital photographs taken at (left to right) baseline and at 1-month posttreatment. At 6 months, the 50-year–old woman showed 24.8% fat reduction, 23.7% muscle thickening, and 8-cm waist circumference reduction.

Conclusion

Simultaneous application of HIFEM and RF is safe and effective for muscle toning and fat reduction. The results suggest this application as more effective for fat reduction and muscle increase than using these energies stand-alone or

consecutively. Further studies are required to support these outcomes.

References

1. Mazzoni D, Lin MJ, Dubin DP, Khorasani H. Review of non-invasive body contouring devices for fat reduction, skin tightening and muscle definition. *Australas J Dermatol* 2019;60:278–83.
2. Kennedy J, Verne S, Griffith R, Falto-Aizpurua L, et al. Non-invasive subcutaneous fat reduction: a review. *J Eur Acad Dermatol Venereol* 2015;29:1679–88.
3. Hoffmann K, Soemantri S, Hoffmann K, Hoffmann KKP. Body shaping with high-intensity focused electromagnetic technology. *J Für Ästhetische Chir* 2020;13:64–9.
4. Weiss RA, Bernardy J. Induction of fat apoptosis by a non-thermal device: mechanism of action of non-invasive high-intensity electromagnetic technology in a porcine model. *Lasers Surg Med* 2019;51: 47–53.
5. Halaas Y, Bernardy J. Mechanism of nonthermal induction of apoptosis by high-intensity focused electromagnetic procedure: biochemical investigation in a porcine model. *J Cosmet Dermatol* 2020; 19:605–11.
6. Kinney BM, Lozanova P. High intensity focused electromagnetic therapy evaluated by magnetic resonance imaging: safety and efficacy study of a dual tissue effect based non-invasive abdominal body shaping: MRI evaluation of electromagnetic therapy. *Lasers Surg Med* 2019;51:40–6.
7. Kakigi R, Naito H, Ogura Y, Kobayashi H, et al. Heat stress enhances mTOR signaling after resistance exercise in human skeletal muscle. *J Physiol Sci* 2011;61:131–40.
8. Kobayashi T, Goto K, Kojima A, Akema T, et al. Possible role of calcineurin in heating-related increase of rat muscle mass. *Biochem Biophys Res Commun* 2005;331:1301–9.
9. Uehara K, Goto K, Kobayashi T, Kojima A, et al. Heat-stress enhances proliferative potential in rat soleus muscle. *Jpn J Physiol* 2004;54: 263–71.
10. Goto K, Okuyama R, Sugiyama H, Honda M, et al. Effects of heat stress and mechanical stretch on protein expression in cultured skeletal muscle cells. *Pflugers Arch* 2003;447:247–53.
11. Yoshihara T, Naito H, Kakigi R, Ichinoseki-Sekine N, et al. Heat stress activates the Akt/mTOR signalling pathway in rat skeletal muscle. *Acta Physiol* 2013;207:416–26.
12. Halevy O, Krispin A, Leshem Y, McMurtry JP, et al. Early-age heat exposure affects skeletal muscle satellite cell proliferation and differentiation in chicks. *Am J Physiol Regul Integr Comp Physiol* 2001; 281:R302–309.
13. Adatto MA, Adatto-Neilson RM, Morren G. Reduction in adipose tissue volume using a new high-power radiofrequency technology combined with infrared light and mechanical manipulation for body contouring. *Lasers Med Sci* 2014;29:1627–31.
14. da Mota PGF, Pascoal AGBA, Carita AIAD, Bø K. Prevalence and risk factors of diastasis recti abdominis from late pregnancy to 6 months postpartum, and relationship with lumbo-pelvic pain. *Man Ther* 2015;20:200–5.
15. Kent DE, Jacob CI. Simultaneous changes in abdominal adipose and muscle tissues following treatments by high-intensity focused electromagnetic (HIFEM) technology-based device: computed tomography evaluation. *J Drugs Dermatol* 2019;18:1098–102.
16. Katz B, Bard R, Goldfarb R, Shiloh A, et al. Ultrasound assessment of subcutaneous abdominal fat thickness after treatments with a high-intensity focused electromagnetic field device: a multicenter study. *Dermatol Surg* 2019;45:1542–8.
17. Boisnic S, Divaris M, Nelson AA, Gharavi NM, et al. A clinical and biological evaluation of a novel, noninvasive radiofrequency device for the long-term reduction of adipose tissue: a clinical and biological evaluation of a novel. *Lasers Surg Med* 2014;46:94–103.
18. Hayre N, Palm M, Jenkin P. A clinical evaluation of a next generation, non-invasive, selective radiofrequency, hands-free, body-shaping device. *J Drugs Dermatol* 2016;15:5.
19. Wanitphakdeedecha R, Sathaworawong A, Manuskiatti W, Sadick NS. Efficacy of multipolar radiofrequency with pulsed magnetic field therapy for the treatment of abdominal cellulite. *J Cosmet Laser Ther* 2017;19:205–9.
20. Chang SL, Huang YL, Lee MC, Chang CH, et al. Combination therapy of focused ultrasound and radio-frequency for noninvasive body contouring in Asians with MRI photographic documentation. *Lasers Med Sci* 2014;29:165–72.
21. Manuskiatti W, Wachirakaphan C, Lektrakul N, Varothai S. Circumference reduction and cellulite treatment with a TriPollar radiofrequency device: a pilot study. *J Eur Acad Dermatol Venereol* 2009; 23:820–7.
22. Kilmer SL, Cox SE, Zelickson BD, Bachelor EP, et al. Feasibility study of electromagnetic muscle stimulation and cryolipolysis for abdominal contouring. *Dermatol Surg* 2020;46:S14–21.

Activation of Skeletal Muscle Satellite Cells by a Device Simultaneously Applying High-Intensity Focused Electromagnetic Technology and Novel RF Technology: Fluorescent Microscopy Facilitated Detection of NCAM/CD56

Aesthetic Surgery Journal
2021, 1–9

DOI: 10.1093/asj/sjab002
www.aestheticsurgeryjournal.com
OXFORD UNIVERSITY PRESS

Yael Halaas, MD; Diane Duncan, MD; Jan Bernardy, PhD; Petra Ondrackova, PhD; and Ivan Dinev, DVM, PhD, DSc

Abstract

Background: Myosatellite cells are myogenic stem cells that can transform to provide nuclei for existing muscles or generate new muscle fibers as documented after extended exercise programs.

Objectives: The authors investigated whether the simultaneous application of High-Intensity Focused Electromagnetic (HIFEM) and Synchrode radiofrequency (RF) affects the levels of satellite cells similarly as the prolonged exercise does to achieve muscle growth.

Methods: Three 30-minute simultaneous HIFEM and Synchrode RF treatments (once a week) were administered over the abdominal area of 5 Large White swine aged approximately 6 months. All animals were anesthetized during the treatments and biopsy acquisition. Biopsies of muscle tissue were collected at baseline, 4 days, 2 weeks, and 1 month post-treatment. After binding the specific antibodies, the NCAM/CD56 levels, a marker of activated satellite cells, were quantified employing the immunofluorescence microscopy technique with a UV lamp.

Results: Examined slices showed a continuous increase in satellite cell levels throughout the study. Four days after the treatment, we observed a 26.1% increase in satellite cells, which increased to 30.2% at 2-week follow-up. Additional histological analysis revealed an increase in the cross-sectional area of muscle fibers and the signs of newly formed fibers of small diameters at 2 weeks after the treatment. No damage to muscle tissue and no adverse effects related to the treatment were observed.

Conclusions: The findings indicate that the simultaneous application of HIFEM and novel Synchrode RF treatment can initiate differentiation of satellite cells to support the growth of existing muscles and, presumably, even the formation of new myofibers.

Editorial Decision date: December 18, 2020; online publish-ahead-of-print January 12, 2021.

Dr Halaas is a plastic and cosmetic surgeon in New York, NY, USA. Dr Duncan is a plastic surgeon in Fort Collins, CO, USA. MVDr Bernardy is a lead researcher at Veterinary Research Institute, Brno, Czech Republic. MVDr Ondrackova is a researcher at Veterinary Research Institute, Brno, Czech Republic. Dr Dinev is a professor of general and clinical pathology, Faculty of Veterinary Medicine, Trakia University, Stara Zagora, Bulgaria.

Corresponding Author:
Dr Yael Halaas, 120 E. 56th St, 8th Floor, Suite 800, New York, NY 10022, USA.
E-mail: halaasyael@gmail.com; Instagram: @drhalaas

It was reported that 60.7% of men and 71.6% of women are dissatisfied with their body shape.[1] As a result, aesthetic medicine is often sought to correct body imperfections. Patients seek surgical as well as non-invasive procedures to improve their body contours.[2] For a long time, physicians' non-surgical treatment options were limited to excessive fat reduction and skin rejuvenation. In 2018, an electromagnetic High-Intensity Focused Electromagnetic (HIFEM) technology opened up an entirely new segment in body contouring due to its unique effects on muscles. Until then, physicians did not have a tool to alter the body musculature non-invasively, which significantly contributes to a toned, firm, and aesthetically pleasing appearance.

The technology is based on the induction of supramaximal muscle contractions not achievable voluntarily. Such intense mechanical stress in the muscle tissue triggers processes to adapt to a higher load. Clinical studies investigating the efficacy of HIFEM showed 15% to 18% muscle thickening of abdominal muscles[3-5] and a 10.3% increase in the volume of gluteal muscles.[6]

Because the HIFEM technology was the first of its kind, further innovations were inevitable and led to the development of a novel technology simultaneously combining HIFEM's muscle conditioning with radiofrequency (RF) heating intended for fat elimination. Under normal circumstances, it is impossible to simultaneously utilize the HIFEM and RF energies due to the interference between the HIFEM alternating magnetic field and the solid RF electrode. This interference induces Eddy currents, which results in the heating of the metallic electrodes. This may cause damage to the device and harm the patient. The device thus employs a novel and patented Synchrode RF electrode that eradicates this interference. The unique interspaced design combines hundreds of microelectrodes that make the electrode transparent to the HIFEM-emitted magnetic fields. The technology (EMSCULPT NEO, BTL Industries Inc, Boston, MA) has been cleared by the US FDA for non-invasive lipolysis (breakdown of fat). Based on the FDA's public database, the clinical trials reviewed by the agency during the registration process[7] showed an average 29.8% reduction in abdominal fat thickness and provided histological evidence of fat cell membrane disintegration. However, this innovation is twofold. Firstly, it ranks the technology among the top tier of non-invasive technologies affecting fat. Secondly, it has been evidenced that muscle tissue heating during muscle work positively affects the muscle response to the workload.[8-11] The synergistic effect of simultaneous delivery of HIFEM and Synchrode RF enhances the muscle hypertrophy. HIFEM-induced mechanical stress and RF-induced heat stress to the muscle leads to the release of heat shock proteins (HSP), signaling molecules that promote muscle protein synthesis and thus enhance the muscle hypertrophy.[12,13] A study by Goto et al[14] documented that the HSP expression is highest when heat and mechanical stress are applied simultaneously, proving the synergy between the 2 energies.

Satellite cells, muscle-derived stem cells, which on activation regenerate and strengthen the existing muscle fibers through differentiation,[15] are also essential for muscle hypertrophy. They are usually activated in response to an intense muscle exercise,[16,17] but it has been found that heating may also lead to their activation.[18] Simultaneous application of Synchrode RF and HIFEM should thus result in high activation of satellite cells and consequent magnification of muscle hypertrophy.

We sought in this study to investigate the effect of the simultaneous application of HIFEM and Synchrode RF energies on the levels of satellite cells through immunofluorescence and to assess any structural changes in the muscle tissue through conventional histology.

METHODS

The study was designed as a prospective single-arm trial and was approved by the IRB of the respective authorized body for veterinary trials (The Ministry of Agriculture of the Czech Republic). A representative of the institution supervised the study execution. The animal care complied with the convention to protect vertebrate animals utilized for experimental and other scientific purposes. The study experiment was carried out in between May 2019 and July 2019.

Study Animals

The study included 5 Large White swine (weight ranging between 78 and 83 kg of live weight) with an average age of 6 months. The animals were stabled at the veterinary institute 1 week before the experiment to acclimate them to the new environment and monitor their condition under the supervision of a veterinarian. The condition and health of the animals were assessed through blood analysis 2 days before the experiment.

Study Experiment

All animals received an active treatment procedure with the investigated device combining the HIFEM procedure and Synchrode RF heating (EMSCULPT NEO, BTL Industries Inc., Stevenage, United Kingdom). The treatment procedure included three 30-minute treatments (one per week) applied over the abdomen. Only the left side was treated, and right side of the animal served as a control area. For the execution of the treatment and biopsy collection, the animals were under general anesthesia to

minimize the stress. Anesthesia (2% propofol) was administered by a veterinarian who determined the dosage. The treated area was shaved with an electric clipper beforehand, and a single applicator, secured by a fixation belt, was applied over the treated area. The intensity was set to 100% for both HIFEM and Synchrode RF. The animals were monitored during the entire treatment procedure.

In Vivo Temperature Measurements

The muscle temperature was monitored during the entire treatment for safety reasons and to rule out any possibility of muscle tissue overheating. A thermal probe (FOT Lab Kit Fluoroptic Thermometer, LUXTRON, Advanced Energy, Denver, CO) was inserted into the muscle tissue utilizing ultrasound guiding (Mindray M5Vet, probe 10L4s) to ensure correct probe placement. Temperature recording was active during the whole procedure, after which the probes were removed.

Tissue Collection

The biopsy samples of muscle tissue were collected at baseline, 4 days, and 2 weeks for the immunofluorescence analysis and conventional histology. At 1 month, additional samples were collected for conventional histology. At baseline, the biopsies were collected only from the control site, opposite to the treated area, to avoid bleeding in the treatment area during the muscle contractions and tissue heating. The post-treatment biopsies were always collected from both the treatment site and the control site, resulting in 60 biopsy samples. Self-contained samples were taken for immunofluorescence analysis and conventional histology. The biopsy collection was performed utilizing a disposable biopsy punch with a diameter of 6 mm.

Tissue Sampling and Processing

On collection, the tissue samples intended for histological analysis were preserved utilizing 10% buffered formalin and fixed in paraffin blocks. The blocks were cut into five 5- to 10-µm-thick slices (175 slices in total) and were stained with hematoxylin and eosin staining. The slices were examined by a certified histopathologist employing light microscopy for any structural changes.

The samples for immunofluorescence were embedded in OCT-cryoprotective embedding medium Tissue Tek (O.C.T. Compound, Sakura-Finetek, Tokyo, Japan) and frozen by supercooled n-heptane placed on dry ice. Then, each tissue sample was cut into four 5- to 10-µm-thick slices (100 slices in total) on the cryostat (Leica Microsystems, CM 1900, GmbH, Wetzlar, Germany) at a temperature of −20°C. Slices were placed on slides and fixed in pre-cooled acetone for 5 minutes and stored at −80°C.

Immunofluorescence aimed to target the NCAM/CD56 marker, which is known for the successful labeling of both quiescent and activated satellite cells and has been utilized by most studies investigating the satellite cells.[19-22] Protein Block (DAKO, Glostrup, Denmark) was applied on the slides to prepare the slides for the analysis, and the slides were then incubated at 37°C in a humid chamber for 30 minutes. Then, anti-Hu CD56, clone MEM-188 (Exbio Praha a.s., Vestec u Prahy, Czech Republic), and anti-Laminin, clone A5 (OriGene Technologies GmbH, Herford, Germany) primary antibodies were applied, and the slides were incubated for 60 minutes at 37°C in a humid chamber. The slides were washed, and goat anti-mouse IgG2a Alexa Fluor 594 (ThermoFisher Scientific, Waltham, MA) and goat anti-rat IgG Alexa Fluor 488 (ThermoFisher Scientific, Waltham, MA) secondary antibodies were added and incubated for 60 minutes at 37°C in a humid chamber. Then, the slides were washed, and Vectashield mounting medium with 4′,6-diamidino-2-phenylindole (Vector Laboratories, Burlingame, CA) was applied.

Evaluation of Satellite Cell Levels

The pre-processed slides were examined at magnifications of 40× and 200× utilizing a fluorescent microscope (Olympus IX51, Tokyo, Japan) with UV-lamp (Olympus u-RFL-T, Tokyo, Japan). A Canon EOS 1100D camera (Tokyo, Japan) and software CellSens Standard software (Den Haag, the Netherlands) were used to capture the slides as images.

The pre-processing procedure ensured that satellite cells were labeled in red, myonuclei as blue, and cell membranes of individual muscle fibers as green. Obtained images were evaluated by utilizing Cell Profiler software that calculates color clusters. The level of satellite cells in each slide was determined as a ratio of labeled satellite cells to the total number of myonuclei. The differences between baseline, post-treatment, and control slides were statistically tested employing a 2-way ANOVA test with a level of significance $\alpha = 0.05$.

Muscle Fiber Size Evaluation

Processed slides were further utilized for evaluation of muscle fiber size. In each slide, the cross-sectional area of individual muscle fibers was measured with ImageJ software, version Fiji.[23] The area of up to 800 muscle fibers was measured for each time point. Obtained values for each time point were clustered into groups according

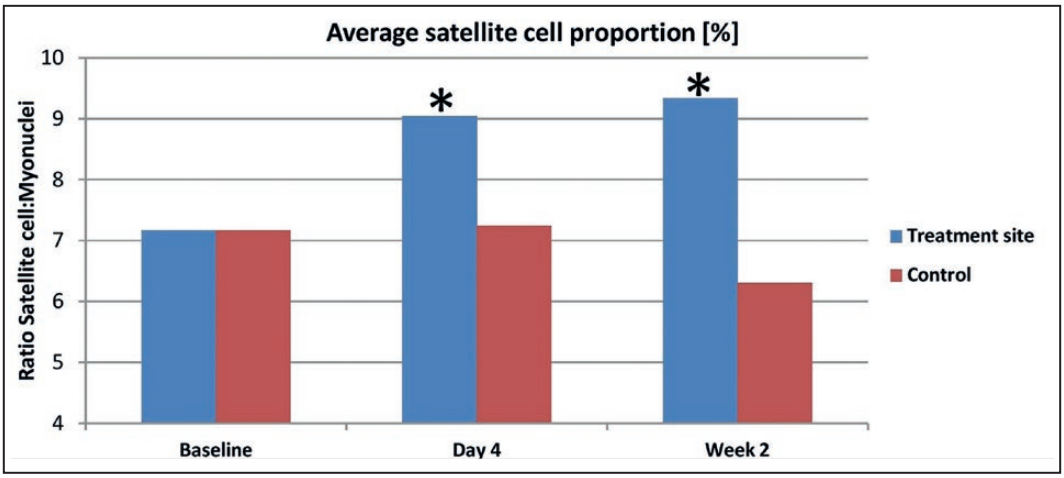

Figure 1. Measured satellite cell proportion at baseline, 4 days, and 2 weeks post-treatment. Statistically significant changes are labeled by asterisk.*

to the size to monitor the fiber size frequency distribution over time.

RESULTS

Pretreatment blood analysis confirmed the good health condition of all pigs. The animals withstood the anesthesia without any complications, and the treatments were well tolerated without any observable side effects. Throughout the experiment, the animals were stabled at the veterinary institute to monitor their health conditions and potential treatment-related complications and side effects. The follow-up sample collection from all animals was administered at exactly 4 days, 14 days, and 30 days after the last treatment. On completion of the experiment and collection of the final biopsies, the animals were euthanized by a certified veterinarian.

Immunofluorescence

The assessment of satellite cell proportion within the stained slides showed a statistically significant ($P < 0.05$) increase by 26.1% on the fourth day after the last treatment. At 2 weeks post-treatment, the level of satellite cells further increased by 30.2% compared with baseline. In absolute values, the satellite cell proportion ($N_{satelite}/N_{myonucleus}$) increased from 0.071 ± 0.012 at baseline to 0.09 ± 0.016 on the fourth day post-treatment and 0.093 ± 0.038 at 2 weeks post-treatment. The same increasing pattern was observed in all of the treated animals. The control samples collected from the opposite site after 4 days (0.072 ± 0.011) and 2 weeks (0.063 ± 0.012) did not show any statistically significant changes from baseline. A detailed comparison of the results is shown in Figure 1, and an example of stained slides captured by a fluorescent microscope is shown in Figure 2.

Histological Examination

A histopathologist examined the histological slides for any structural changes in the muscle tissue. The post-treatment slices obtained after 4 days did not show visually noticeable structural changes. However, at 2 weeks, the muscle tissue showed enlarged hypertrophic fibers, with the most prominent enlargement seen at 1 month post-treatment. At 1 month, the muscle tissue showed apparent hypertrophic changes compared with baseline, accompanied by a decreased intramuscular sheaf space, as shown in Figure 3.

The histological slides did not show any deviations from normal healthy muscle structure, and no signs of muscle tissue damage or adverse events were observed. A few samples did contain blood hemorrhage, which is something that cannot be entirely avoided during the invasive nature of biopsy sample collection. Lastly, several slices of the muscle tissue collected 1 month post-treatment showed structures that were not present at baseline slices and appeared to be newly formed muscle fibers (see Figure 4).

Muscle Fiber Size Measurements

The baseline measurements showed that the majority (69%) of all fibers ranged between 2000 and 6000 μm^2, whereas only 17% were smaller and only 14% exceeded 6000 μm^2. After the treatments, a significant shift in the distribution has been seen: the ratio of small muscle fibers increased from 17% to 21% at 2 weeks post-treatment and to 22% at 1 month post-treatment. Similarly, the ratio of large

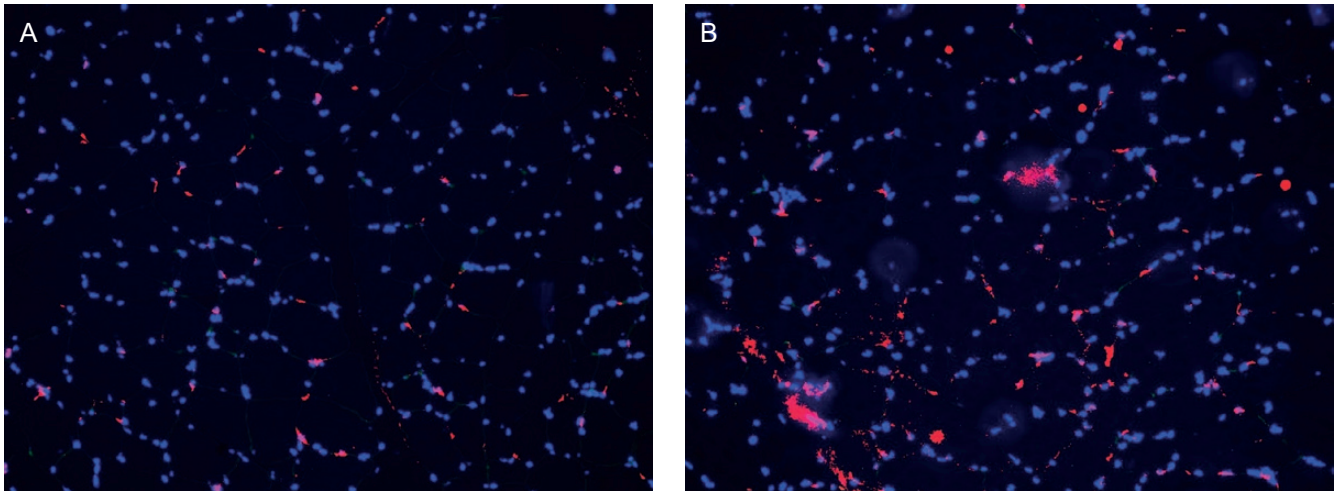

Figure 2. (A) An Example of the stained slides of baseline (B) and 2-week muscle tissue viewed under a fluorescent microscope. The satellite cells are colored by red and myonuclei by blue.

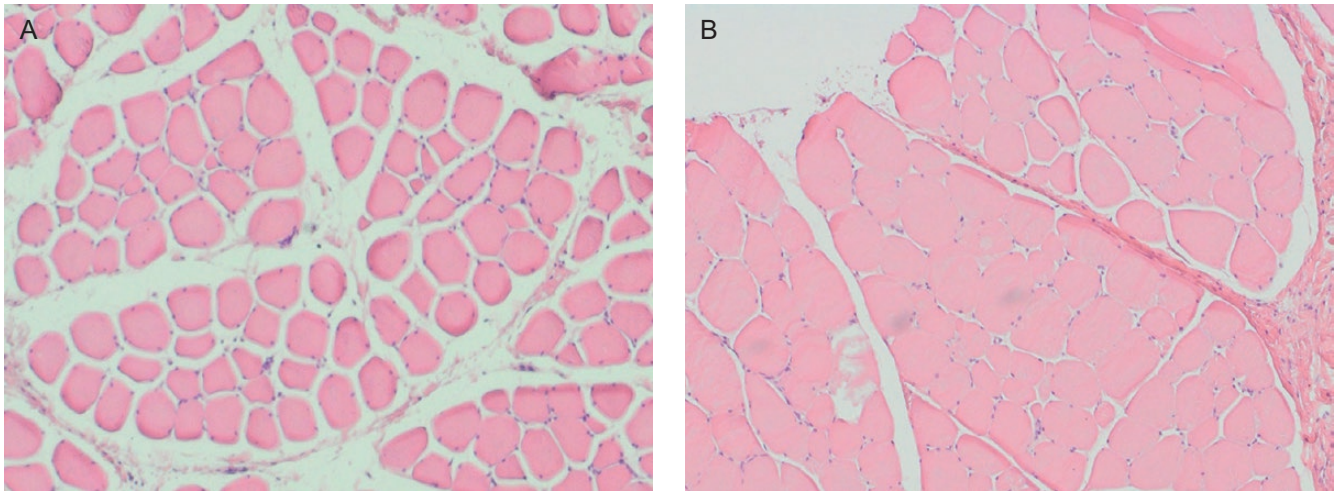

Figure 3. (A) An example of the histology images of muscle tissue collected at baseline (B) 1 month post-treatment. The post-treatment tissue shows hypertrophic fibers and a noticeable increase in the muscle tissue with decreased intramuscular sheaf space.

hypertrophic cells increased from 14% at baseline to 29% at 2 weeks and even up to 33% at 1 month. Control measurements at 1 month did not show any significant fluctuation in the distribution compared with baseline. The detailed results can be seen in Figure 5, where the frequency ratio of each size group is displayed.

Temperature Monitoring

On initiation of the treatment, the muscle temperature quickly increased from 38°C to 40°C in only 2 minutes. The temperature was then maintained between 40° and 41°C for the entire treatment. Throughout the treatment, the temperature did not exceed 41°C and was constant without any large fluctuations, ensuring therapy safety (Figure 6). for the muscle temperature graph during the treatment.

DISCUSSION

The study investigated the effect of the simultaneous application of HIFEM and Synchrode RF energies on muscle tissue. The results showed a significant increase in satellite cell levels, which play a vital role in the tissue adaptive response to the muscle work. These observations were coupled with hypertrophic changes seen in the histological slides.

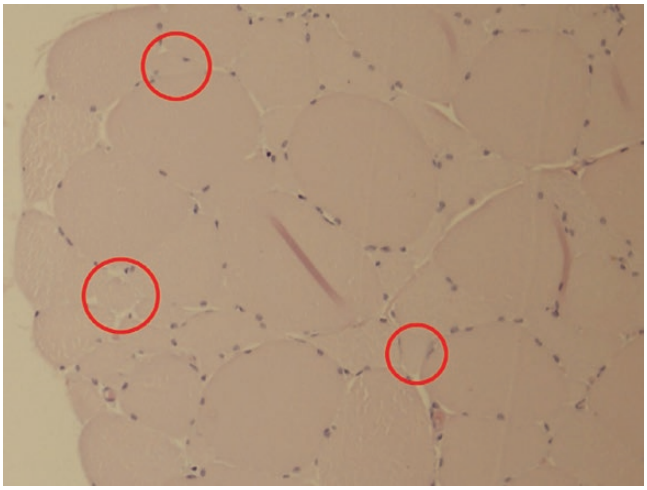

Figure 4. The red circles mark the area with muscle fibers of small diameter that may indicate newly formed muscle fibers at histology slice collected 1 month post-treatment.

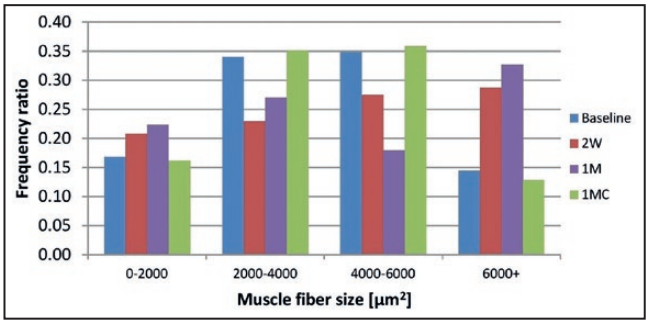

Figure 5. Frequency distribution of muscle fiber size at baseline, 2 weeks (2W), 1 month (1M), and 1 month control (1MC).

Satellite cells are usually activated by intense muscle exercise to regenerate and strengthen the existing muscle fibers. However, it has been found that heating also activates satellite cells.[18] It is unknown whether the application of both types of stimuli leads to differentiation of the satellite cells, but higher levels of active satellite cells increase the chances of differentiation. Comparing our findings with previous studies[24-26] investigating the satellite cell levels post-exercise showed that the 30.2% increase after 3 sessions of HIFEM + RF treatment was comparable and even exceeded the activation levels seen after 12 to 16 weeks of intense exercise programs. The detailed comparison is shown in Table 1. Although a portion of the investigational treatment results may be associated with the supramaximal nature of HIFEM contractions, this comparison strongly indicates the importance of controlled heating during the contractions. The role of heating on muscle tissue has already been documented in studies investigating HSPs, signaling molecules promoting muscle protein synthesis.[12,13,27,28] Studies found that HSPs can be activated by mechanical stress (intense muscle contraction) as well as by heat stress of 40°C to 41°C. A study comparing the effect of such heat stress, mechanical stress, and simultaneously applied heat and mechanical stress showed the highest muscle protein synthesis when the heat and mechanical stress were applied simultaneously.[14]

An equivalent temperature within the 40°C to 41°C range was also measured throughout the whole procedure in our study. Thus, the conditions were very similar to those in the studies mentioned above and may explain the high activation of satellite cells. The temperature did not exceed 41°C. It was stable for the entire treatment time, which is important for safety reasons because a temperature of 42°C may be potentially harmful to the muscle.[29]

Unfortunately, to date, there is no established way of measuring the level of differentiation of satellite cells. It is not possible to determine whether the differentiation would result in the formation of new muscle fibers or new myonuclei to support the existing muscle fibers. This is the reason why the histological assessment was also included. The slide observations were in agreement with the satellite cell results as notable hypertrophic changes were seen, most prominent at 1 month post-treatment. No damage or harmful reaction of tissue was present in the slides, further confirming the treatment safety. Aside from hypertrophic changes, the post-treatment slides showed structural formations that appeared to be newly formed muscle fibers, which would suggest that some of the satellite cells differentiated into new fibers. Although not statistically significant, signs of hyperplasia post HIFEM treatments have already been documented in a study by Duncan at al.[30] Our histological and immunofluorescence observations strongly support the premise put forth in the previous paper that HIFEM directly causes both muscle hyperplasia and hypertrophy.

The results of muscle fiber size measurements showed an increased number of large hypertrophic fibers on post-treatment slides, indicating that the treatment triggered hypertrophic changes in the tissue as the fibers grew in time and the frequency ratio of large fibers increased by 135.7% from 0.14 at baseline to 0.33 at 1 month. Aside from fiber growth, the number of small-diameter fibers was increased on post-treatment slides compared with baseline or control. The frequency ratio of small fibers increased by 29.4% from 0.17 at baseline to 0.22 at 1 month. This finding strongly suggests muscle fiber hyperplasia as an answerable phenomenon explaining this increase. Hyperplasia hypothesis corresponds to the observation of increased levels of activated myosatellite cells, which may in fact differentiate to form new muscle fibers. Yet, the number of small fibers did not further increase at 1 month compared with the 2-week measurements. A possible explanation could be a continuous growth of these fibers, which are thus allocated into

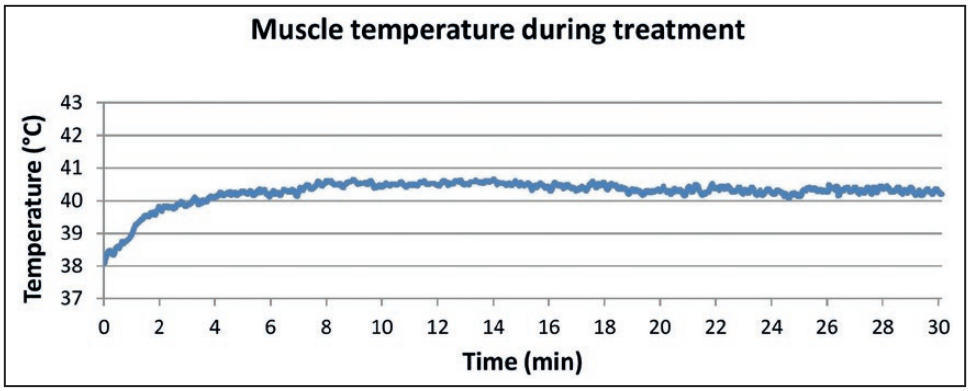

Figure 6. The graph shows the measured rapid temperature elevation in the first 2 minutes from 38°C to 40°C and a stable temperature within the 40°C to 41°C range for the rest of the treatment.

Table 1. Comparison of Results With Studies Investigating the Effect of Exercise on Satellite Cell Levels

Study	Program	Satellite cell content
Current study	3 sessions HIFEM+RF	+30.2%
Mackey et al[24]	12 weeks exercise (females)	+18%
Mackey et al[24]	12 weeks exercise (males)	+36%
Olsen et al[25]	16 weeks exercise	+27%
Olsen et al[25]	4 weeks exercise	+22%
Kadi et al[26]	30 days exercise	+19%
Kadi et al[26]	90 days exercise	+31%

HIFEM+RF, procedure delivering high-intensity focused electromagnetic and radiofrequency simultaneously.

different size group at 1 month. Newly formed fibers between 2 weeks and 1 month thus represent the same ratio.

Limitations of this study include a relatively low sample size of 5 animals utilized due to ethical reasons to minimize the number of experimental animals. To compensate for the smaller sample size, each tissue sample was cut into 5 to 10 slices (depending on the evaluation method), which increased the statistical power. Another limitation of this study is the short-term follow-up limited to 1 month. However, the goal of this study was to investigate immediate tissue response to supramaximal contractions in adjunction with heating. Monitoring longevity of these outcomes should be a subject of further research. The utilization of a single marker for satellite cells could also be considered as a limitation. However, the collected samples' preparation process did not allow the application of more markers; therefore, the most commonly employed marker NCAM/CD56 was chosen. Furthermore, the utilization of an animal model itself is a limitation because a human tissue response may show some discrepancies. It is known that the relative distribution of skeletal muscle fiber types differs between humans and pigs: human muscle tissue contains 50% to 65% of type I fibers, whereas pig muscle tissue contains only 9% to 11%.[31] It could thus be argued that the results observed in this study may not be transferable to humans, and in fact the applicability of these results should be evaluated in humans as well. However, the properties of the magnetic stimuli such as frequency, pulse duration, or pulse shape delivered during the HIFEM treatments were designed to be able contract both types of fibers. Moreover, the results of pilot studies[32,33] investigating the simultaneous delivery of HIFEM and RF document greater muscle thickening effect (24.2%-26.1%) than that of HIFEM only treatments[3,34] (14.8%-15.4%), which suggests our results may be applicable to humans. Further research including human patients should be conducted to verify the outcomes.

This was the first trial, to our knowledge, to investigate the effects of the simultaneous application of HIFEM and Synchrode RF heating on muscle tissue. Future studies should include comparison with consequent or individual treatments. To fully understand the synergy between heat and HIFEM-induced mechanical stress, it would be beneficial to investigate the HSP phenomenon with HIFEM and Synchrode RF and its correlation with existing research. Further research is also necessary to examine the longevity of the results, and longer follow-ups should thus be included. Lastly, we believe that the signs of hyperplasia should be further investigated.

CONCLUSIONS

The simultaneous application of HIFEM and Synchrode RF energies significantly enhances the levels of satellite pool

and results in muscle hypertrophy and likely in muscle hyperplasia. The results of 3 treatments are comparable with programs involving 12 to 16 weeks of intense exercise, making the technology a convenient tool for enhancing muscle mass that could be highly attractive for body contouring purposes.

Disclosures

Dr Duncan and Dr Halaas are medical advisors for BTL Industries Inc. (Stevenage, United Kingdom). The other authors declared no potential conflicts of interest with respect to the research, authorship, and publication of this article.

Funding

The authors received no financial support for the research, authorship, and publication of this article.

REFERENCES

1. Kruger J, Lee C-D, Ainsworth BE, Macera CA. Body size satisfaction and physical activity levels among men and women. *Obesity*. 2008;16(8):1976-1979.
2. The Aesthetic Society's Cosmetic Surgery National Data Bank: Statistics 2019. *Aesthet Surg J*. 2020;40(S1):1-26.
3. Kent DE, Jacob CI. Simultaneous changes in abdominal adipose and muscle tissues following treatments by high-intensity focused electromagnetic (HIFEM) technology-based device: computed tomography evaluation. *J Drugs Dermatol*. 2019;18(11):1098-1102.
4. Kinney BM, Lozanova P. High intensity focused electromagnetic therapy evaluated by magnetic resonance imaging: safety and efficacy study of a dual tissue effect based non-invasive abdominal body shaping. *Lasers Surg Med*. 2019;51(1):40-46.
5. Kinney BM, Kent DE. MRI and CT assessment of abdominal tissue composition in patients after high-intensity focused electromagnetic therapy treatments: one-year follow-up. *Aesthet Surg J*. 2020;40(12):NP686-NP693.
6. American Society for Laser Medicine and Surgery 2019 late breaking abstracts. *Lasers Surg Med*. 2019;51(S31): S4-S15.
7. US Food and Drug Administration. 510(k) premarket notification: K192224. Published online December 5, 2019. https://www.accessdata.fda.gov/cdrh_docs/pdf19/K192224.pdf. Accessed June 30, 2020.
8. Shellock FG, Prentice WE. Warming-up and stretching for improved physical performance and prevention of sports-related injuries. *Sports Med*. 1985;2(4):267-278.
9. Giombini A, Giovannini V, Di Cesare A, et al. Hyperthermia induced by microwave diathermy in the management of muscle and tendon injuries. *Br Med Bull*. 2007;83:379-396.
10. Gogte K, Srivastav P, Miyaru GB. Effect of passive, active and combined warm up on lower limb muscle performance and dynamic stability in recreational sports players. *J Clin Diagn Res*. 2017;11(3):YC05-YC08.
11. Racinais S, Cocking S, Périard JD. Sports and environmental temperature: from warming-up to heating-up. *Temperature (Austin)*. 2017;4(3):227-257.
12. Kakigi R, Naito H, Ogura Y, et al. Heat stress enhances mTOR signaling after resistance exercise in human skeletal muscle. *J Physiol Sci*. 2011;61(2):131-140.
13. Yoshihara T, Naito H, Kakigi R, et al. Heat stress activates the Akt/mTOR signalling pathway in rat skeletal muscle. *Acta Physiol (Oxf)*. 2013;207(2):416-426.
14. Goto K, Okuyama R, Sugiyama H, et al. Effects of heat stress and mechanical stretch on protein expression in cultured skeletal muscle cells. *Pflugers Arch*. 2003;447(2):247-253.
15. Mauro A. Satellite cells of skeletal muscle fibers. *J Cell Biol*. 1961;9(2):493-495.
16. Moss FP, Leblond CP. Satellite cells as the source of nuclei in muscles of growing rats. *Anat Rec*. 1971;170(4):421-435.
17. Schultz E, McCormick KM. Skeletal muscle satellite cells. *Rev Physiol Biochem Pharmacol*. 1994;123:213-257.
18. Halevy O, Krispin A, Leshem Y, McMurtry JP, Yahav S. Early-age heat exposure affects skeletal muscle satellite cell proliferation and differentiation in chicks. *Am J Physiol Regul Integr Comp Physiol*. 2001;281(1):R302-R309.
19. Kadi F, Eriksson A, Holmner S, Butler-Browne GS, Thornell LE. Cellular adaptation of the trapezius muscle in strength-trained athletes. *Histochem Cell Biol*. 1999;111(3):189-195.
20. Maier F, Bornemann A. Comparison of the muscle fiber diameter and satellite cell frequency in human muscle biopsies. *Muscle Nerve*. 1999;22(5):578-583.
21. Kadi F. Adaptation of human skeletal muscle to training and anabolic steroids. *Acta Physiol Scand Suppl*. 2000;646:1-52.
22. Illa I, Leon-Monzon M, Dalakas MC. Regenerating and denervated human muscle fibers and satellite cells express neural cell adhesion molecule recognized by monoclonal antibodies to natural killer cells. *Ann Neurol*. 1992;31(1):46-52.
23. Schindelin J, Arganda-Carreras I, Frise E, et al. Fiji: an open-source platform for biological-image analysis. *Nat Methods*. 2012;9(7):676-682.
24. Mackey AL, Esmarck B, Kadi F, et al. Enhanced satellite cell proliferation with resistance training in elderly men and women. *Scand J Med Sci Sports*. 2007;17(1):34-42.
25. Olsen S, Aagaard P, Kadi F, et al. Creatine supplementation augments the increase in satellite cell and myonuclei number in human skeletal muscle induced by strength training. *J Physiol*. 2006;573(Pt 2):525-534.
26. Kadi F, Schjerling P, Andersen LL, et al. The effects of heavy resistance training and detraining on satellite cells in human skeletal muscles. *J Physiol*. 2004;558(Pt 3):1005-1012.
27. Uehara K, Goto K, Kobayashi T, et al. Heat-stress enhances proliferative potential in rat soleus muscle. *Jpn J Physiol*. 2004;54(3):263-271.
28. Kobayashi T, Goto K, Kojima A, et al. Possible role of calcineurin in heating-related increase of rat muscle mass. *Biochem Biophys Res Commun*. 2005;331(4):1301-1309.

29. Dewhirst MW, Viglianti BL, Lora-Michiels M, Hoopes PJ, Hanson M. Thermal dose requirement for tissue effect: experimental and clinical findings. *Proc SPIE Int Soc Opt Eng*. 2003;4954:37.
30. Duncan D, Dinev I. Noninvasive induction of muscle fiber hypertrophy and hyperplasia: effects of high-intensity focused electromagnetic field evaluated in an in-vivo porcine model: a pilot study. *Aesthet Surg J*. 2020;40(5):568-574.
31. Bode G, Clausing P, Gervais F, et al.; Steering Group of the RETHINK Project. The utility of the minipig as an animal model in regulatory toxicology. *J Pharmacol Toxicol Methods*. 2010;62(3):196-220.
32. Jacob C, Kent DE. Abdominal toning and reduction of subcutaneous fat with combination of HIFEM procedure and radiofrequency treatment. Conference Proceedings of the Annual Meeting of the American Society for Dermatologic Surgery. October 2020;8-11.
33. Katz BE, Samuels JB, Weiss RA. Novel radiofrequency device used in combination with HIFEM procedure for abdominal body shaping: sham-controlled randomized trial. Conference Proceedings of the Annual Meeting of the American Society for Dermatologic Surgery. October 2020;8-11.
34. Kinney BM, Lozanova P. High intensity focused electromagnetic therapy evaluated by magnetic resonance imaging: safety and efficacy study of a dual tissue effect based non-invasive abdominal body shaping. *Lasers Surg Med*. 2019;51(1):40-46.

SYNCHRONIZED RF & HIFEM: ULTRASOUND EVALUATION OF FAT TISSUE

ULTRASOUND EVALUATION OF THE SIMULTANEOUS RF AND HIFEM TREATMENTS ON HUMAN FAT TISSUE

Radina Denkova MD[1]

1. Aesthetic Clinic Beauty, Sofia, BG

Source: U.S. Food and Drug Administration. 510(k) Premarket Notification: K192224.Published online December 5, 2019.

HIGHLIGHTS

- **Reduction** in **subcutaneous fat thickness** at 3 months was **29.8%**.
- A total of **88.1%** of patients **were satisfied** with treatment outcomes.
- **92.9%** of patients found the treatments **comfortable**.
- Waist **circumference** was **reduced** on average **by 3.2 cm**.

BASELINE

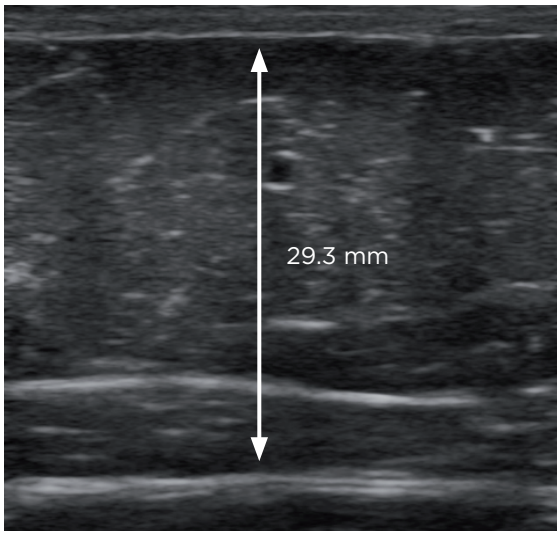

3 MONTHS AFTER

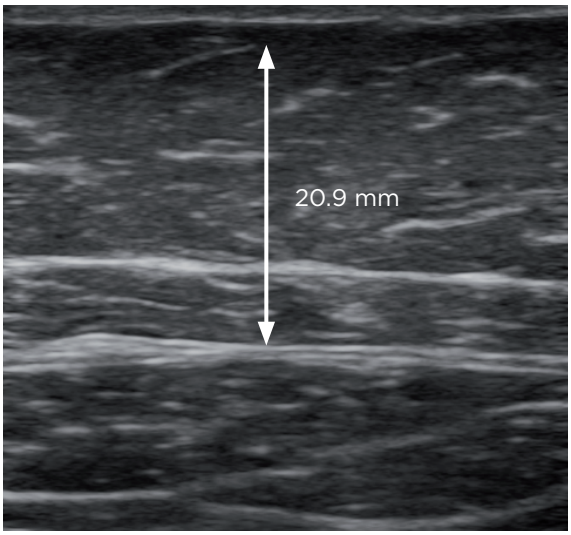

Ultrasound images of a 42-year old female, who also showed a 4-cm reduction in waist circumference.

STUDY DESIGN

- 42 subjects (29 females, 13 males).
- Three 30-minute treatments on abdomen.
- Evaluation by ultrasound imaging.

RESULTS

- Results showed continuous improvement over time.

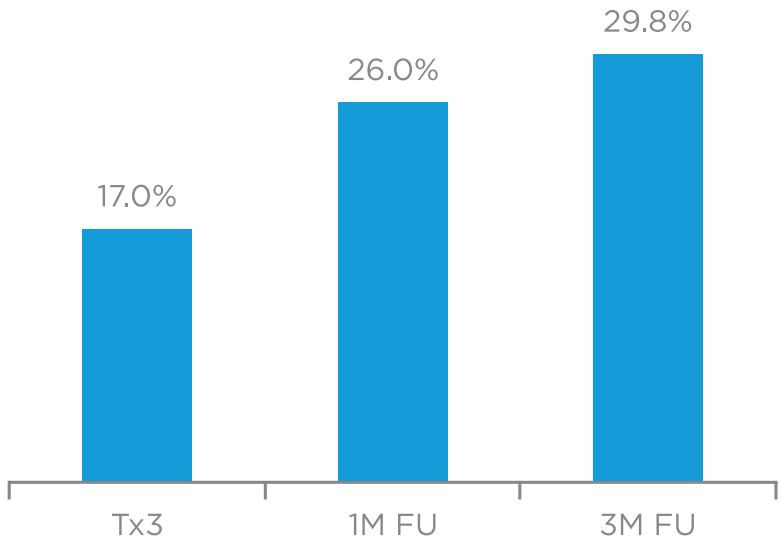

The chart showing continuous improvement in the fat reduction over time.

BASELINE

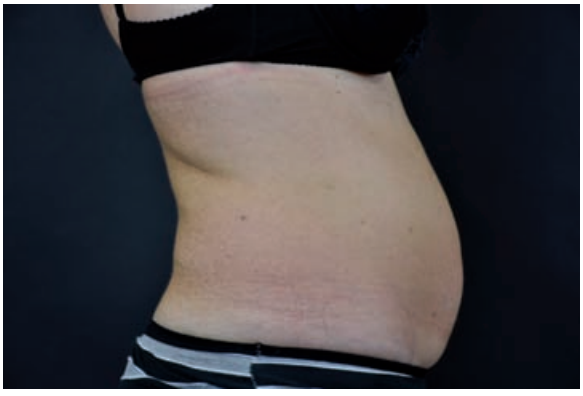

3 MONTHS AFTER

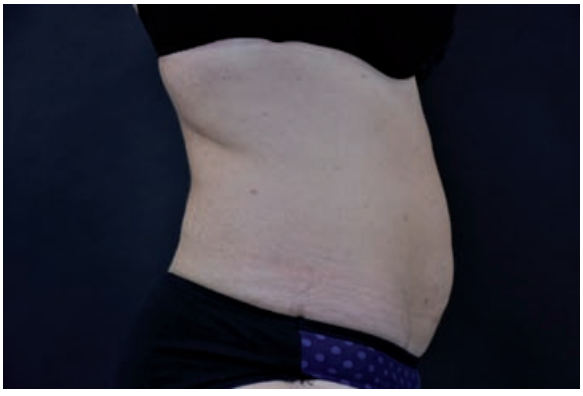

A 49-year old female at baseline and 3 months post-treatment showing 4.5 cm waist circumference reduction and 29.2% reduction in abdominal fat layer.

SYNCHRONIZED RF & HIFEM: MULTI-CENTER ABDOMINAL ULTRASOUND STUDY

RADIOFREQUENCY HEATING AND HIFEM DELIVERED SIMULTANEOUSLY - THE FIRST SHAM-CONTROLLED RANDOMIZED TRIAL

Bruce Katz MD[1], Robert Weiss MD[2], Julene B. Samuels MD[3] F.A.C.S

1. Juva Skin and Laser Center, Manhattan, NY, USA; 2. Maryland Laser Skin & Vein Institute, Hunt Valley, MD, USA; 3. Julene B Samuels MD. F.A.C.S, Louisville, KY, USA

Presented at the Annual Meeting of the American Society for Dermatologic Surgery, 2020 Virtual Meeting.

HIGHLIGHTS

- A total of 72 subjects allocated into two groups (Active: N=48, **BMI of 25.8 kg/m2)**; Sham: N=24, **BMI of 25.6 kg/m2)**.
- Active group showed **28.3% reduction in subcutaneous fat** at **3-month** follow-up visit.
- **Muscle thickness** increased by **24.2%** at **3-months** post-treatment in **active group**.
- At 3 months **38/40 patients** showed fat reduction **higher than 20%**.

A 64-YEAR OLD FEMALE

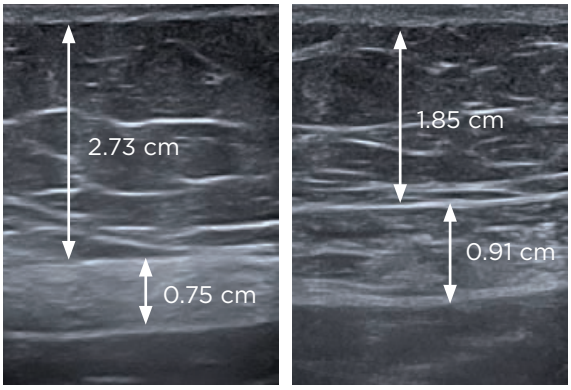

A 51-YEAR OLD FEMALE

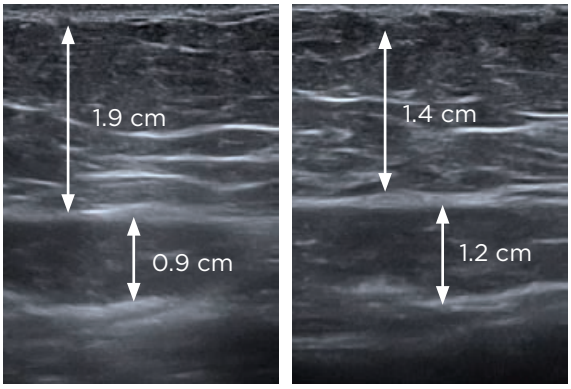

Ultrasound images of patients in active group taken before (left) and 1 month after (right) the treatments.

STUDY DESIGN

- Both groups received three 30-minute treatments on abdomen (active: maximum tolerable intensities, sham: intensities of 5%).
- Ultrasound images were taken at baseline, 1M and 3M after the last treatment.
- Evaluation included measurements of subcutaneous fat and muscle mass thickness.

CONCLUSION

- **Dual field technology** showed **high efficacy** for subcutaneous **fat reduction** and thickening of **rectus abdominis muscle**.
- **93.9%** of patients reported satisfaction with the results.
- **Sham treatments did not induce** any **significant changes**.
- **The procedure** combining HIFEM and RF energy **was safe** and did not cause any adverse events.

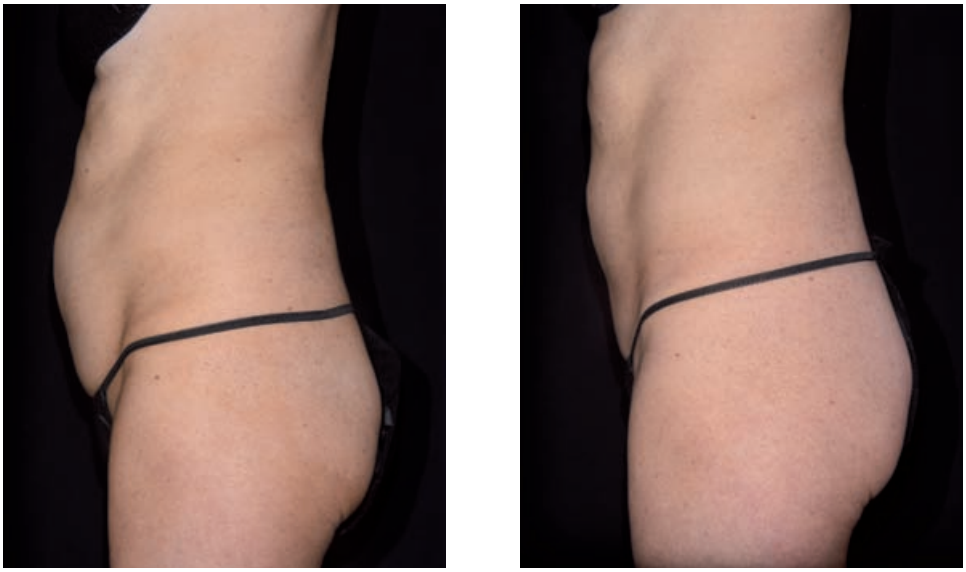

Digital photographs of a 55-year old female, taken before (left) and 3 months after (right) the treatments.

SYNCHRONIZED RF & HIFEM: HISTOLOGICAL EVALUATION OF THE EFFECT ON FAT IN HUMANS

HISTOLOGICAL EVALUATION OF THE SIMULTANEOUS RF AND HIFEM TREATMENTS ON HUMAN FAT TISSUE

Radina Denkova MD.

1. Aesthetic Clinic Beauty, Sofia, BG

Source: U.S. Food and Drug Administration. 510(k) Premarket Notification: K192224.Published online December 5, 2019.

HIGHLIGHTS

- **Intensive fat cell disruption peaking at 20 days post-treatment**.
- **Non-invasive lipolysis** seen in the **first 10 days** post-treatment.
- Investigated device was found to be effective for **elimination of fat cells**.
- **No damage** to skin, sweat glands and sebaceous glands was observed, ensuring procedural safety.
- **Deformed nucleus** and pyknotic nucleus indicating **cell death**.

BASELINE

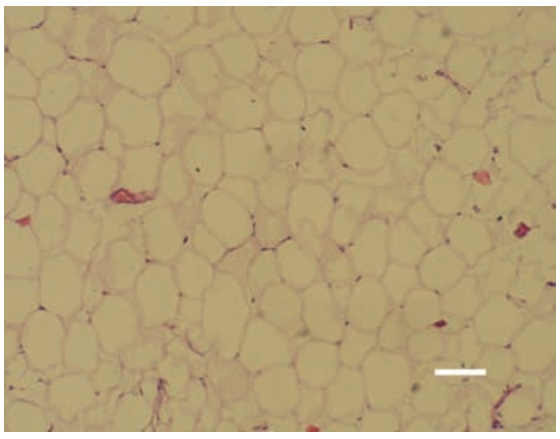

20 DAYS AFTER

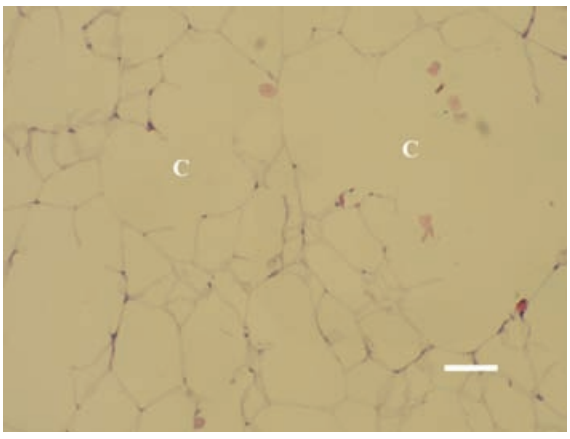

Normal subcutaneous tissue morphology with typical uniform size of adipocytes at the left; bar = 40 micrometers. Intensive fat cell disruption (C) and alternation of adipocytes shape 20 days post-treatment at the right; bar = 30 micrometers.

899-74EMCNSBCA4EN100
Emsculpt_Neo_LF_Studybook-Cover_A4_EN100
07/2021